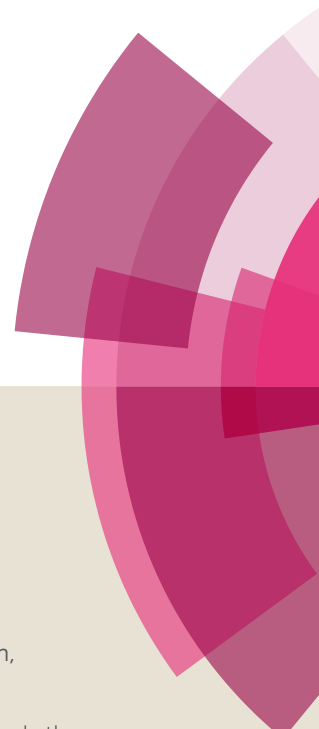


MedChemComm

Accepted Manuscript



This article can be cited before page numbers have been issued, to do this please use: C. Maguire, Z. Chen, V. Mocharla, M. Sriram, T. Strecker, E. Hamel, H. Zhou, R. Lopez, Y. Wang, R. Mason, D. J. Chaplin, M. Trawick and K. G. Pinney, *Med. Chem. Commun.*, 2018, DOI: 10.1039/C8MD00322J.



This is an Accepted Manuscript, which has been through the Royal Society of Chemistry peer review process and has been accepted for publication.

Accepted Manuscripts are published online shortly after acceptance, before technical editing, formatting and proof reading. Using this free service, authors can make their results available to the community, in citable form, before we publish the edited article. We will replace this Accepted Manuscript with the edited and formatted Advance Article as soon as it is available.

You can find more information about Accepted Manuscripts in the [author guidelines](#).

Please note that technical editing may introduce minor changes to the text and/or graphics, which may alter content. The journal's standard [Terms & Conditions](#) and the ethical guidelines, outlined in our [author and reviewer resource centre](#), still apply. In no event shall the Royal Society of Chemistry be held responsible for any errors or omissions in this Accepted Manuscript or any consequences arising from the use of any information it contains.

Synthesis of dihydronaphthalene analogues inspired by combretastatin A-4 and their biological evaluation as anticancer agents.

Casey J. Maguire ^a, Zhi Chen ^a, Vani P. Mocharla ^a, Madhavi Sriram ^a, Tracy E. Strecker ^a, Ernest Hamel ^b, Heling Zhou ^c, Ramona Lopez ^c, Yifan Wang ^a, Ralph P. Mason ^c, David J. Chaplin ^{a,d}, Mary Lynn Trawick ^a, Kevin G. Pinney ^{a,*}

^a *Department of Chemistry and Biochemistry, Baylor University, One Bear Place #97348, Waco, TX 76798-7348, United States of America*

^b *Screening Technologies Branch, Developmental Therapeutics Program, Division of Cancer Treatment and Diagnosis, National Cancer Institute, Frederick National Laboratory for Cancer Research, National Institutes of Health, Frederick, MD 21702, United States of America*

^c *Department of Radiology, The University of Texas Southwestern Medical Center, 5323 Harry Hines Boulevard, Dallas, TX 75390-9058, United States of America*

^d *Mateon Therapeutics, Inc., 701 Gateway Boulevard, Suite 210, South San Francisco, CA 94080, United States of America*

*Corresponding author. Tel.: (254) 710-4117; E-mail address: Kevin_Pinney@baylor.edu

Dedication:

Dedicated to the memory of Dr. Anjan Ghatak, an inspiring and creative synthetic organic, medicinal chemist who made seminal contributions to the science described in this manuscript.

Animal Care and Use Statement:

All animal procedures were approved by the University of Texas Southwestern Medical Center Institutional Animal Care and Use Committee under APN101222 and 102169.

Abstract

The natural products colchicine and combretastatin A-4 (**CA4**) have provided inspiration for the discovery and development of a wide array of derivatives and analogues that inhibit tubulin polymerization through a binding interaction at the colchicine site on β -tubulin. A water-soluble phosphate prodrug salt of **CA4** (referred to as **CA4P**) has demonstrated the ability to selectively damage tumor-associated vasculature and ushered in a new class of developmental anticancer agents known as vascular disrupting agents (VDAs). Through a long-term program of structure activity relationship (SAR) driven inquiry, we discovered that the dihydronaphthalene molecular scaffold provided access to small-molecule inhibitors of tubulin polymerization. In particular, a dihydronaphthalene analogue bearing a pendant trimethoxy aryl ring (referred to as **KGP03**) and a similar aroyl ring (referred to as **KGP413**) were potent inhibitors of tubulin polymerization ($IC_{50} = 1.0$ and $1.2 \mu\text{M}$, respectively) and displayed low nM cytotoxicity against human cancer cell lines. In order to enhance water-solubility for *in vivo* evaluation, the corresponding phosphate prodrug salts (**KGP04** and **KGP152**, respectively) were synthesized. In a preliminary *in vivo* study in a SCID-BALB/c mouse model bearing the human breast tumor MDA-MB-231-luc, a 99% reduction in signal was observed with bioluminescence imaging (BLI) 4 h after IP administration of **KGP152** (200 mg/kg) indicating reduced tumor blood flow. In a separate study, disruption of tumor-associated blood flow in a Fischer rat bearing an A549-luc human lung tumor was observed by color Doppler ultrasound following administration of **KGP04** (15 mg/kg).

1. Introduction

The natural products colchicine¹ and combretastatin A-4 (**CA4**)^{2,3} provide a rich canopy for SAR-guided molecular interrogation directed towards the discovery of highly potent inhibitors of tubulin polymerization (Fig. 1). This rich, natural products-based structural landscape has enabled the exploration of a wide range of structural diversity, resulting in literally thousands of synthetic analogues and derivatives with structural and functional group modifications of both aryl rings and the ethylene bridge of **CA4**.⁴⁻⁹ Key structural features of the combretastatins include the trimethoxy phenyl ring, the *p*-methoxyphenyl moiety, *cis*-configuration of the aromatic rings and a distance of approximately 4-5 Å between the aryl rings.^{5,9,10} Our long-standing research agenda in this area has contributed a variety of functionalized molecular scaffolds including benzo[*b*]thiophene¹¹⁻¹³ indole,^{12,14-18} benzofuran,^{12,15,19} stilbenoid,^{5,9,20-22} and benzosuberene analogues²³⁻²⁶ that bear structural analogy to colchicine and **CA4**. Our original molecular design motif recognized salient aspects of structural similarity between non-steroidal,¹¹ anti-estrogen agents (such as nafoxidine and LY117018)^{27,28} and **CA4**, which led us to the discovery of a collection of highly potent inhibitors of tubulin polymerization that function through a direct binding interaction at the colchicine site on the tubulin heterodimer.^{12,13,21,23-26,29,30} In addition to functioning as antiproliferative (cytotoxic agents), colchicine site inhibitors of tubulin polymerization can also function as vascular disrupting agents (VDAs). Selective disruption of tumor-associated microvessels results in loss of nutrients, oxygen deprivation, and ultimately necrosis.³¹⁻³⁸ Therefore, this therapeutic approach offers a unique and promising strategy for the treatment of cancer, which is mechanistically distinct from that of the angiogenesis inhibiting agents (AIAs),³⁹ such as bevacizumab (AvastinTM)⁴⁰ that target the angiogenesis process.³¹⁻³⁴ The sub-set of colchicine site inhibitors of tubulin polymerization that function as VDAs induce rapid morphological changes (flat to round) in the endothelial cells lining microvessels, leading to microvessel occlusion, compromised vessel wall integrity, and necrosis.^{33,36,41-43} VDAs are selective for tumor-associated neovasculature due to the primitive nature of these vessels, which are typically incomplete or missing basement membranes, deficient in smooth muscle and pericytes, and therefore more reliant on endothelial cells to maintain the shape of the vessel wall.^{16,44-48}

Herein, we report the design, synthesis, and preliminary biological evaluation of a 5-hydroxy-6-methoxy-1-aryldihydronaphthalene analogue (referred to as **KGP03**, Fig. 1) along with its corresponding 1-aryldihydronaphthalene analogue (referred to as **KGP413**, Fig. 1). Functionalized dihydronaphthalene analogues of this nature bear structural similarity to **CA4** and have been previously reported by us^{5,21,25,49-53} and others.⁵⁴ Our previous studies with indole analogues (such as OXi8006) along with Pettit's discovery of phenstatin (synthetic benzophenone analogue of **CA4**, Fig. 1)^{55,56} confirmed the tolerability (and potential benefit) of a carbonyl group juxtaposed between functionalized aryl rings in regard to

inhibition of tubulin polymerization, cytotoxicity, and *in vivo* efficacy. These molecules along with **CA4** have very limited water-solubility, and in their initial development of the combretastatins, Pettit and co-workers astutely developed phosphate prodrug salts of **CA4** and **CA1** (referred to as **CA4P** and **CA1P**, respectively) that dramatically increased water-solubility (Fig. 1).^{57–59} This strategy has also been applied to these dihydronaphthalene analogues to generate water-soluble phosphate prodrug salts (**KGP04** and **KGP152**, respectively, Fig. 1). Synthetic strategies towards these molecules are reported along with inhibition of tubulin polymerization (cell-free assay) and cytotoxicity against NCI-H460 (non-small cell lung carcinoma), DU-145 (prostate carcinoma), and SK-OV-3 (ovarian adenocarcinoma) human cancer cell lines. The two water-soluble prodrugs (**KGP04** and **KGP152**) were subjected to preliminary *in vivo* (mouse and rat) evaluation to assess their ability to disrupt tumor-associated vasculature and thus function as VDAs.

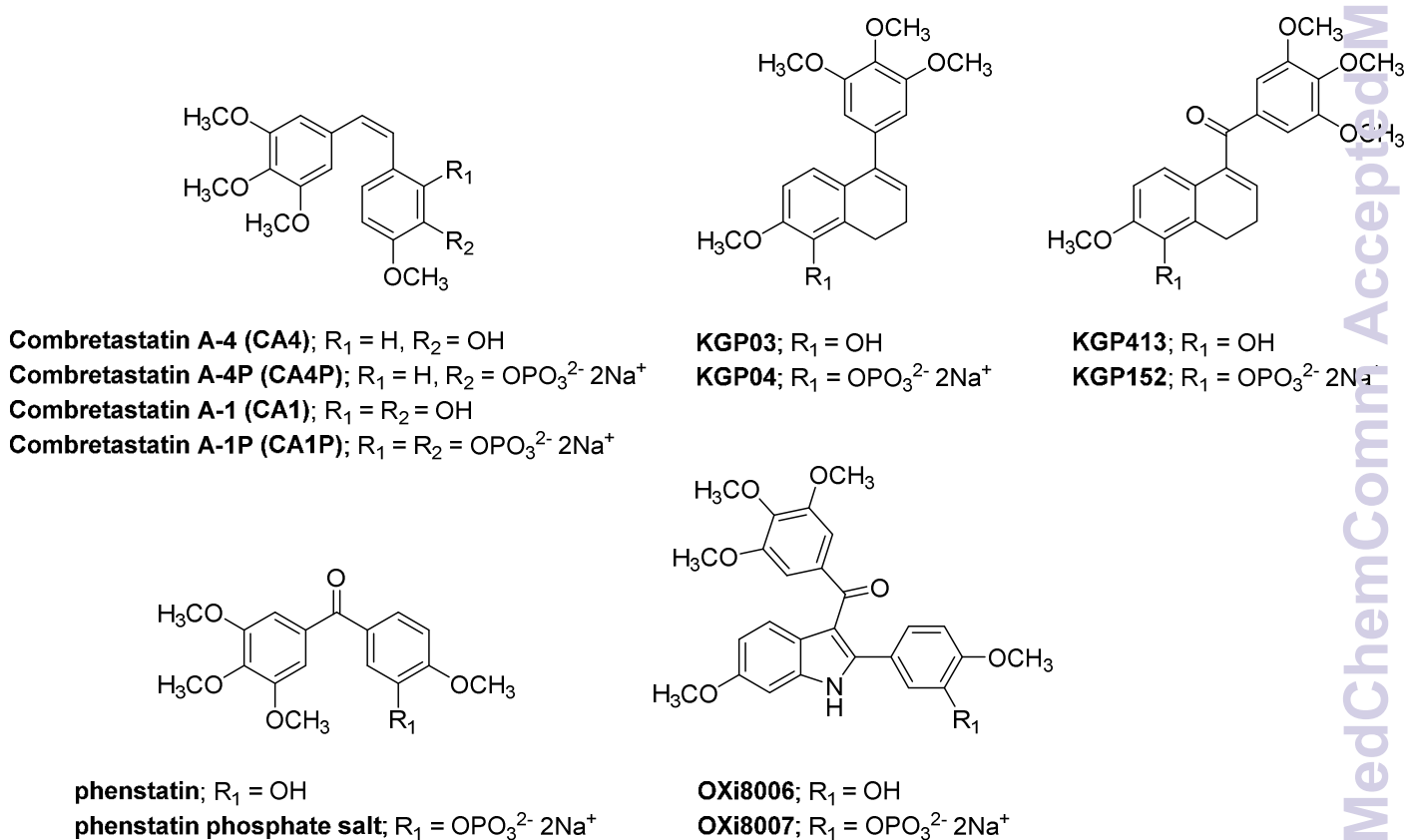


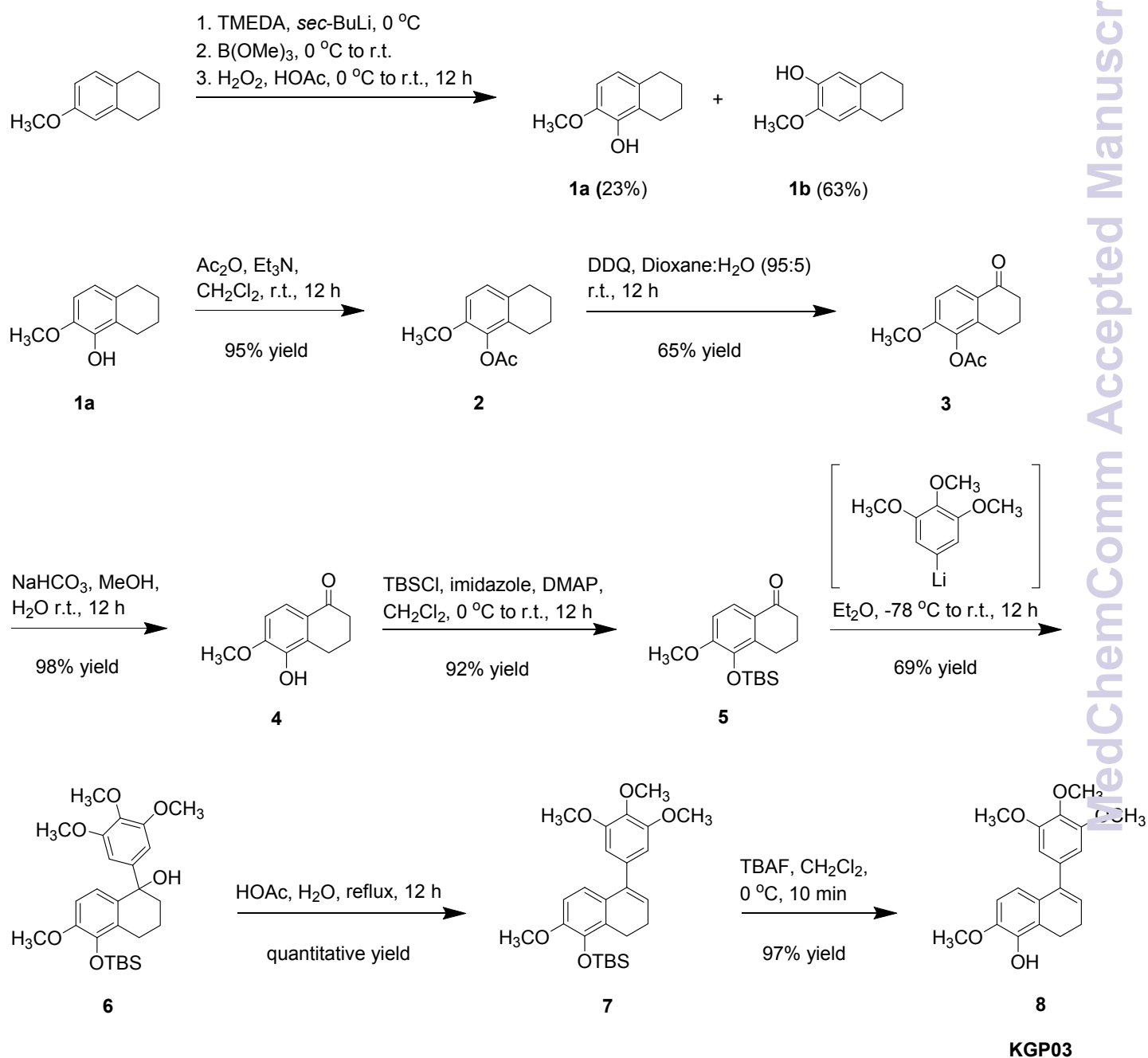
Figure 1. Representative small-molecule inhibitors of tubulin assembly that bind to the colchicine site; including the combretastatin analogues (**CA4**, **CA1**),^{2,3} dihydronaphthalene analogues (**KGP03** and **KGP413**), isocombretastatin analogue **phenstatin**,^{55,56} and indole analogue (**OXi8006**), along with the corresponding phosphate salt prodrugs.

2. Results and discussion

2.1. Synthesis

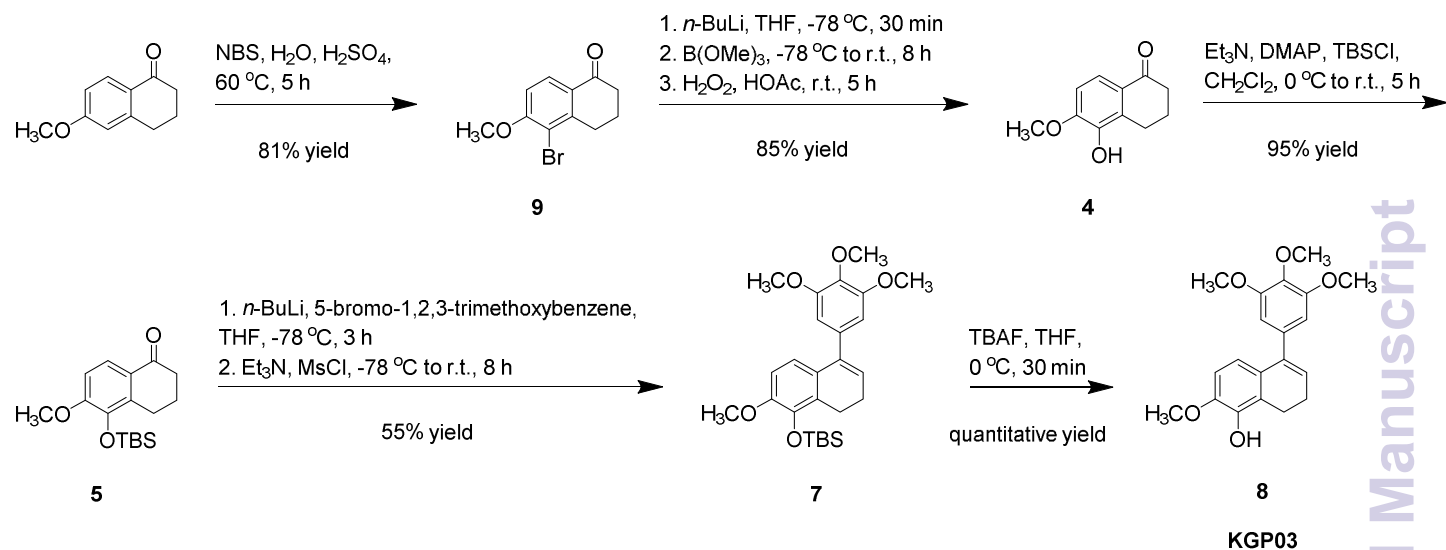
Our initial synthetic route towards **KGP03** (Scheme 1) provided the target compound in a 9% overall yield from 6-methoxytetralin.^{21,25,49,54} Considering an alternative strategy to the synthesis of **KGP03** in order to improve efficiency and overall yield, 6-methoxy-1-tetralone was selected as a starting material (Scheme 2). This precursor is more advanced, commercially available, and approximately half the cost of the tetralin used in the original synthesis. Regioselective bromination of the tetralone followed by lithium halogen exchange provided a means to direct the hydroxylation to the regiochemically desired position in a significantly higher yield (69% for 2 steps) compared to the *ortho*-directed C-H deprotonation of tetralin used in the original route (23% yield for 1 step).^{25,60,61} The phenolic tetralone **4** was subsequently converted to its corresponding silyl ether **5** upon treatment with TBSCl. Installation of the trimethoxy aryl ring and elimination of the resulting tertiary alcohol to generate **KGP03** was accomplished in a one-pot reaction. The appropriate aryllithium intermediate (prepared *in situ* from the corresponding aryl bromide) was allowed to react with tetralone **5**, and the resulting tertiary alcohol (*in situ*) was treated with triethylamine and mesyl chloride to furnish the KGP03-silyl ether derivative **7**.⁶² Desilylation with TBAF afforded **KGP03** in a 5-step synthesis with a 36% overall yield.

Our initial route to the carbonyl hinged analogue, **KGP413**, centered on a modified Shapiro coupling reaction (Scheme 3). Ketone **5** was converted to hydrazine **10**, which provided the *in situ*



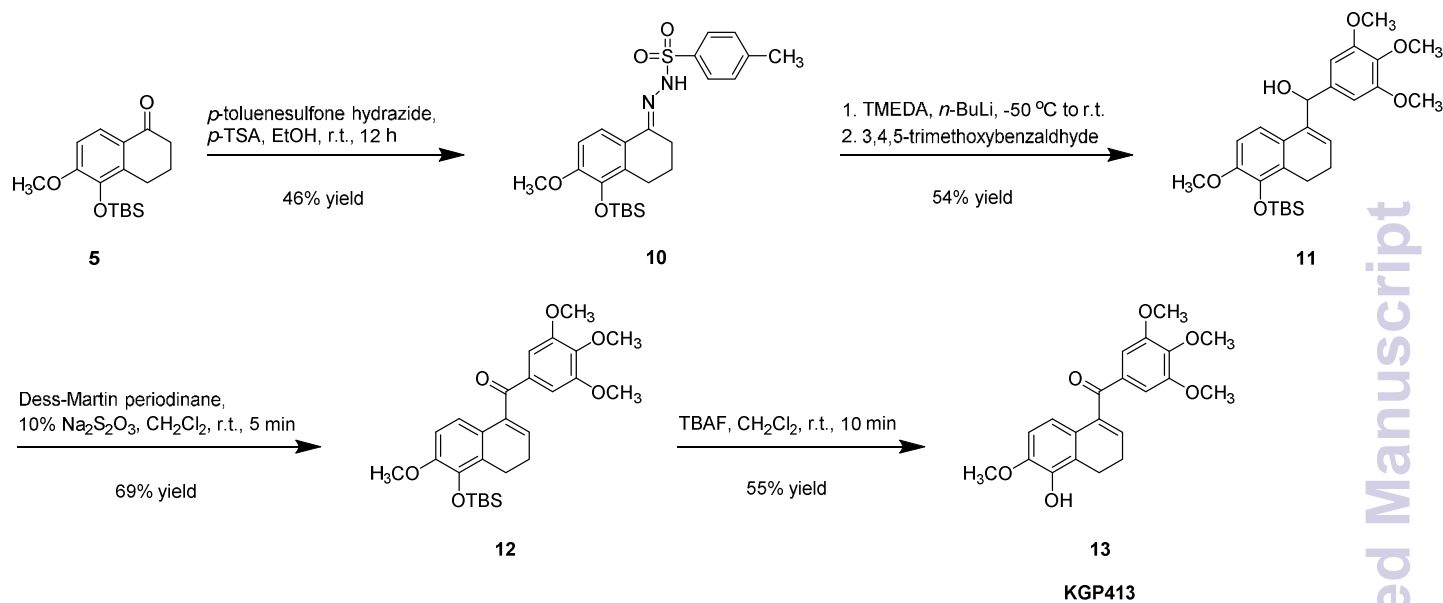
Scheme 1. Synthesis of **KGP03** from 6-Methoxytetralin Featuring Early Installation of Phenolic Moiety

generated vinyl lithium adduct that was subsequently treated with 3,4,5-trimethoxybenzaldehyde to afford secondary alcohol **11**. Dess-Martin oxidation provided silyl-ether derivative **12**, which was desilylated to

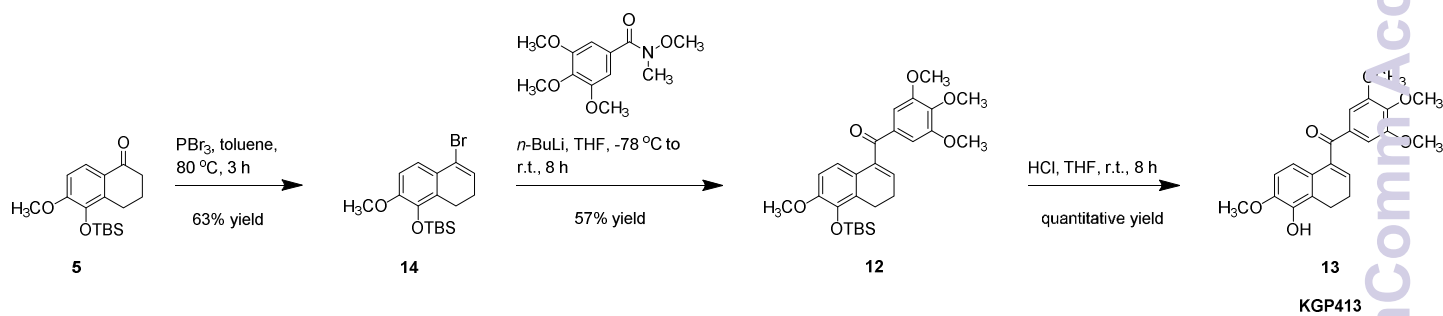


Scheme 2. Efficient Alternative Synthesis of **KGP03** from 6-Methoxytetralone afford **KGP413**.^{25,49} Our improved synthesis of **KGP413** (Scheme 4), proceeded through a silyl ether tetralone intermediate that was highlighted in the **KGP03** synthesis (Scheme 2). The ketone was converted to vinyl bromide **14** using phosphorus tribromide.⁶³ The corresponding vinyl lithium intermediate was prepared *in situ* followed by the addition of the trimethoxy aryl Weinreb amide to afford silyl-ether derivative **12**. Desilylation using concentrated HCl afforded **KGP413** in a 6-step synthesis with a 23% overall yield. This was a significant improvement from the original 9-step synthesis that resulted in a 1% overall yield.

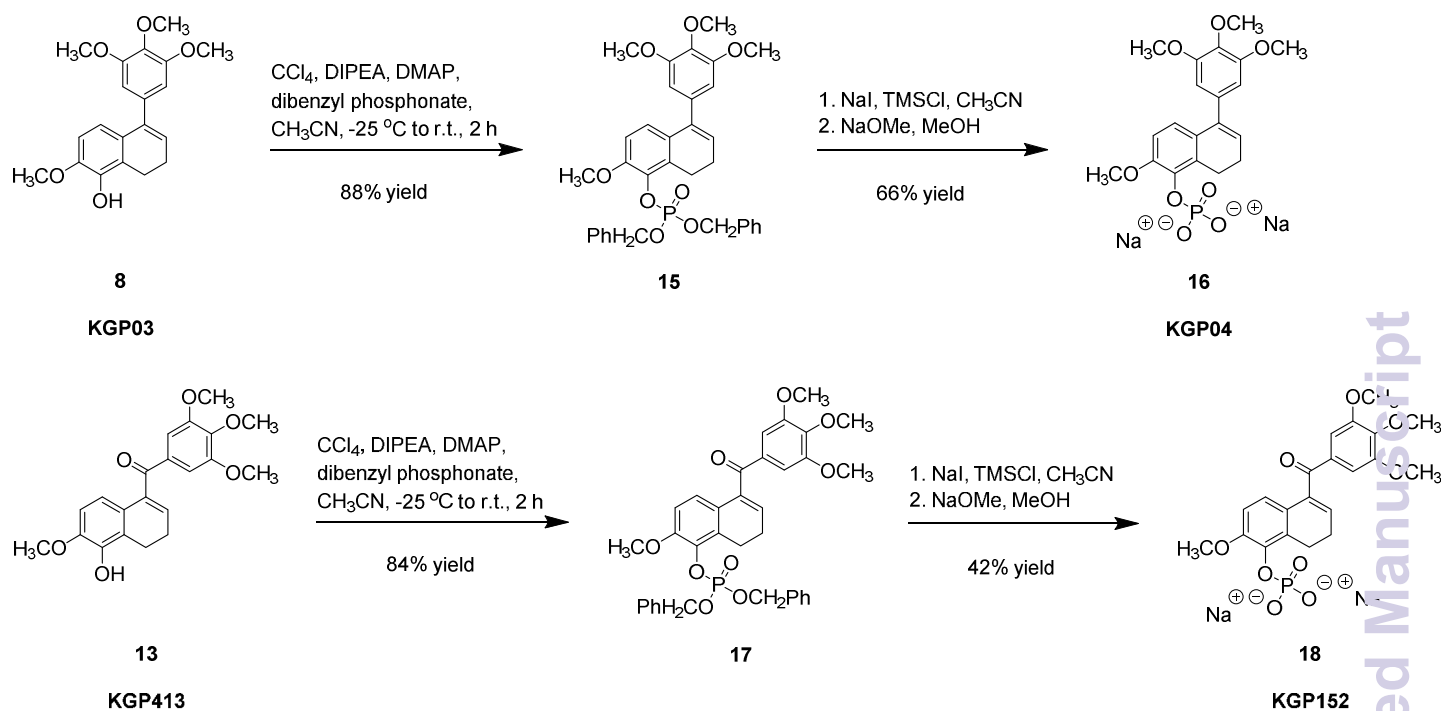
The reaction of either phenol (**8** or **13**) with *in situ*-generated dibenzyl chlorophosphite resulted in the expected dihydronaphthalene dibenzyl phosphate ester derivative (**15** or **17**, Scheme 5). Debenzylation was accomplished using *in situ*-generated iodomethylsilane, from chloromethylsilane and sodium iodide. The *in situ*-generated TMS-phosphate ester intermediate was quenched using sodium methoxide in methanol to afford the disodium phosphate salt prodrug (**16** or **18**).^{22,57}



Scheme 3. Synthesis of KGP413 from 6-Methoxytetralin Featuring a Modified Shapiro Coupling Reaction



Scheme 4. Efficient Alternative Synthesis of KGP413 from 6-Methoxytetralone Featuring a Weireb Amide Coupling Reaction



Scheme 5. Synthesis of **KGP04** and **KGP152** phosphate prodrug salts

2.2. Biological evaluation

The two phenolic dihydronaphthalene analogues (**KGP03** and **KGP413** along with their corresponding water-soluble phosphate prodrug salts **KGP04** and **KGP152**) were evaluated for their ability to inhibit the polymerization of purified tubulin. Both **KGP03** and **KGP413** were potent inhibitors ($IC_{50} = 0.46$ and $0.85 \mu\text{M}$, respectively) akin to **CA4** ($IC_{50} = 1.2 \mu\text{M}$) while their corresponding phosphate prodrug salts were inactive ($IC_{50} > 20 \mu\text{M}$), as anticipated, since this cell free assay is devoid of phosphatase enzymes required for cleavage and regeneration of the parent phenolic analogues. Phosphate prodrug salts of this type are typically substrates for alkaline phosphatase enzymes, readily available *in vivo*. We confirmed that **KGP04** underwent conversion (essentially quantitative) to its corresponding phenol (**KGP03**) in the presence of alkaline phosphatase (see Supplemental data file for details). All four dihydronaphthalene compounds demonstrated low nM cytotoxicity (range of 2-52 nM) against the three cancer cell lines utilized in this study, and thus were comparable to the activity of **CA4** and **CA4P**. In order to assess the ability of these compounds to interfere with tumor-associated vasculature and thus function as VDAs, the two water-soluble prodrugs were evaluated against *in vivo* models (mouse and rat) of human cancer (breast and lung, respectively).

Table 1. Inhibition of tubulin polymerization, percent inhibition of colchicine binding, and cytotoxicity of the target dihydronaphthalene analogues

Compound	Inhibition of tubulin polymerization IC ₅₀ (μM) ± SD	% inhibition of colchicine binding ± SD	GI ₅₀ (μM) SRB assay		
			NCI-H460	DU-145	SK-OV-3
KGP03	0.46 ± 0.007	90% ± 2 (1 μM), 98% ± 0.3 (5 μM)	0.00451 ± 0.00104	0.00336 ± 0.000587	0.00219 ± 0.000267
KGP04	> 20	nd ^a	0.00373 ± 0.000851	0.00327 ± 0.00139	0.00190 ± 0.000427
KGP413	1.2 ± 0.007	81% ± 2 (1 μM), 98% ± 2 (5 μM)	0.0216 ± 0.0227	0.00730 ± 0.00869	0.00622 ± 0.00296
KGP152	> 20	nd ^a	0.0524 ± 0.0137	0.0126 ± 0.0125	0.0129 ± 0.0139
CA4 ^b	1.2 ± 0.05	84% ± 1.1 (1 μM), 98% ± 0.1 (5 μM)	0.00500 ± 0.000359	0.00602 ± 0.000661	0.00506 ± 0.00145
CA4P ^c	> 20	nd ^a	0.00282 ± 0.000497	0.00336 ± 0.00105	0.00188 ± 0.000970

a: nd = not determined; b: data from reference 21; c: data from reference 24

Preliminary *In Vivo* Evaluation of Water-Soluble Prodrugs KGP04 and KGP413 as VDAs

The dynamic and longitudinal effect of VDAs can be assessed with various non-invasive imaging modalities.^{38,64} Bioluminescence imaging (BLI) is a widely used optical imaging technique for preclinical research. The light emission of BLI is based on the expression of the luciferase enzyme and the presence of the substrate luciferin. The effect of VDAs can be observed through reduced delivery of substrate luciferin and consequent diminished light emission, as has been demonstrated with several VDAs.^{17,38,41,42,65} We performed a preliminary dose escalation study on three BALB/c SCID mice with orthotopic MDA-MB-231-luc tumors with respective doses of 100, 150, and 200 mg/kg **KGP152** administered IP. Vascular shutdown at 4 hrs following **KGP152** was quite uniform with all three tumors showing at least 85% decrease in light emission. Figure 2 shows the respective decrease of BLI signal 4 and 24 hrs after administration of **KGP152** (200 mg/kg). While dynamic BLI is very effective at revealing vascular disruption, it does require transfected tumor cells to express luciferase. As an alternative, ultrasound can reveal blood flow^{14,38,66,67} and color-Doppler based on the Doppler effect has been previously applied to demonstrate vascular shutdown following the administration of VDAs.¹⁴ Figure 3 shows an example of the use of color-Doppler ultrasound to evaluate the reduction of blood flow 2 h after administration of **KGP04** to a nude rat with a subcutaneous A549 human lung tumor growing in the leg.

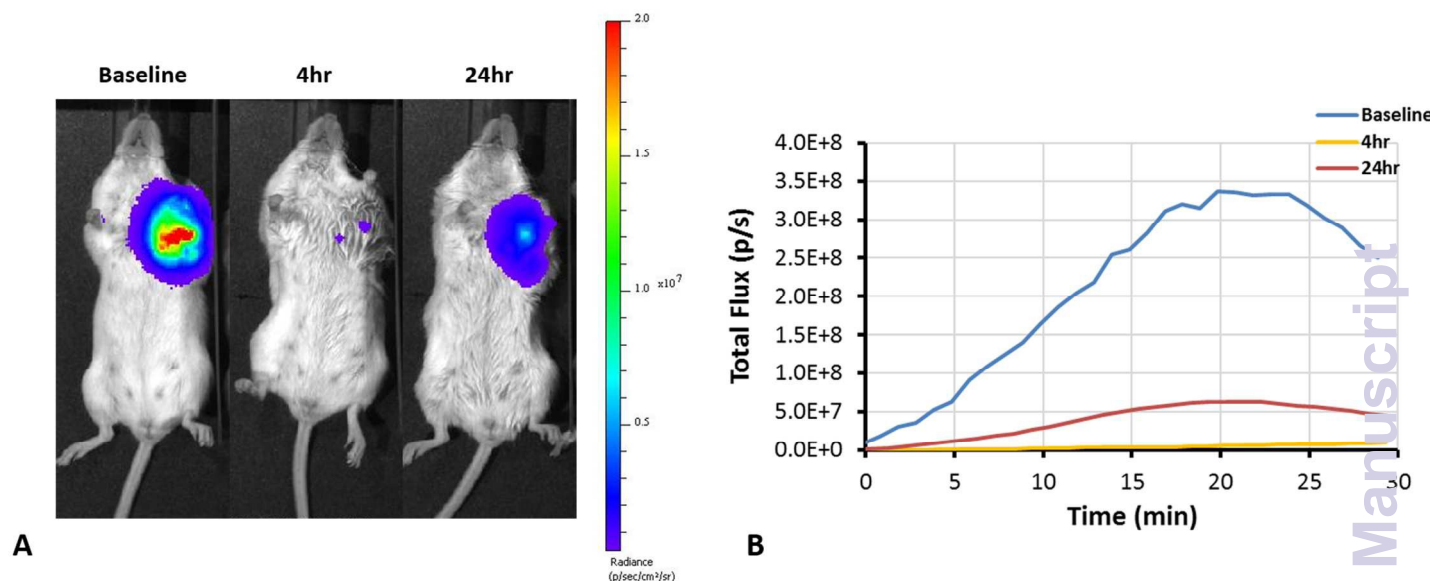


Figure 2. BLI monitoring of tumor response to **KGP152**. **KGP152** (200 mg/kg) was administered IP to a BALB/C SCID mouse with a large MDA-MB-231-luc orthotopic breast tumor (2 cm^3). (A) Images show signal intensity heat maps overlaid on gray scale photographs of mouse at successive time points. Following **KGP152** administration, the BLI signal was dramatically lower at 4 hr (99% signal reduction) and recovered slightly at 24 hr (81% signal reduction from baseline). (B) Corresponding dynamic time courses of total flux obtained following luciferin administration at the three time points.

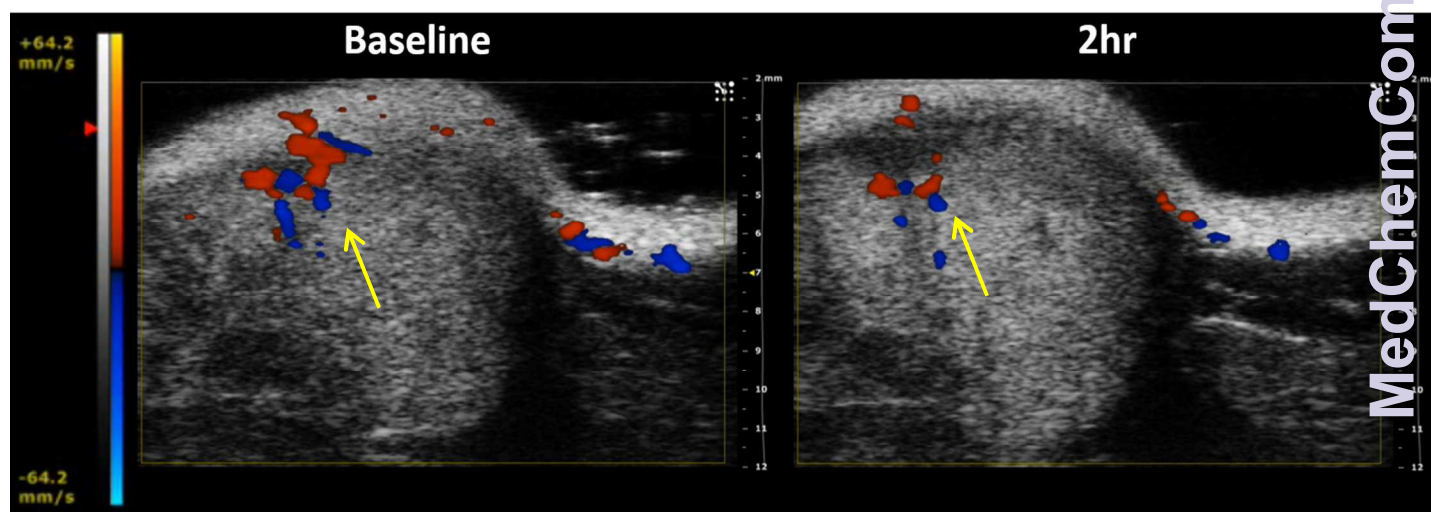


Figure 3. Color Doppler ultrasound images show reduction of tumor blood perfusion. Images show baseline and 2 hr after the administration of **KGP04** (15 mg/kg, IP) to a nude rat with a subcutaneous A549 human tumor xenograft (0.5 cm^3). Red and blue indicate magnitude of flow into and out of plane.

The layer of skin is apparent at the top of the images, together with structural heterogeneity in the tumor. Vascular shutdown is indicated by yellow arrow.

3. Conclusion

In summary, we utilized the dihydronaphthalene molecular scaffold to design and synthesize two promising inhibitors of tubulin polymerization (**KGP03** and **KGP413**) and their corresponding water-soluble phosphate prodrug salts. Initial synthetic routes were further optimized towards these lead compounds. The analogues were evaluated for inhibition of tubulin polymerization and for their ability to compete for colchicine binding, which provided robust data [similar to **CA4** (positive control compound)] for both phenolic dihydronaphthalene compounds (**KGP03** and **KGP413**). Potent cytotoxicity (low nM GI₅₀ values) was observed for the four compounds (**KGP03/KGP04** and **KGP413/KGP152**) against the three human cancer cell lines (NCI-H460, DU-145, and SK-OV-3) used in this study. Preliminary *in vivo* BLI evaluation of dihydronaphthalene prodrug **KGP152** (200 mg/kg) against an MDA-MB-231-luc orthotopic breast tumor (SCID mouse model) showed a dramatic decrease in signal after 4 h. The signal recovered only slightly after 24 h. Preliminary *in vivo* assessment (nude rat bearing the A549 tumor) of **KGP04** (15 mg/kg) demonstrated evidence of vascular shutdown (imaged by color Doppler ultrasound). Thus, these dihydronaphthalene analogues appear to be promising candidates for further development as antiproliferative agents and VDAs.

4. Experimental section

4.1. Chemistry

4.1.1. General materials and methods

Dichloromethane, methanol, diethylether, and tetrahydrofuran (THF) were used in their anhydrous forms, as obtained from the chemical suppliers. Reactions were performed under an inert nitrogen atmosphere. Thin-layer chromatography (TLC) plates (precoated glass plates with silica gel 60 F254, 0.25 mm thickness) were used to monitor reactions. Purification of intermediates and products was carried out with a Biotage Isolera flash purification system using silica gel (200-400 mesh, 60 Å) or manually in glass columns. Intermediates and products synthesized were characterized on the basis of their ¹H NMR (600, 500 MHz), ¹³C NMR (151 or 126 MHz) spectroscopic data using a Bruker Avance III 600 MHz or a Varian VNMRs 500 MHz instrument. Spectra were recorded in CDCl₃, CD₃OD, or C₃D₆O. All chemical shifts are expressed in ppm (δ), coupling constants (*J*) are presented in Hz, and peak patterns are reported as singlet (s), doublet (d), triplet (t), quartet (q), septet (sept), double doublet (dd), and multiplet (m).

Purity of the final compounds was further analyzed at 25 °C using an Agilent 1200 HPLC system with a diode-array detector ($\lambda = 190\text{-}400$ nm), a Zorbax XDB-C18 HPLC column (4.6 mm x 150 mm, 5 μm), and a Zorbax reliance cartridge guard-column; method A: solvent A, acetonitrile, solvent B, 0.1% TFA in H₂O; or method B: solvent A, acetonitrile, solvent B, H₂O; gradient, 10% A/90% B to 100% A/0% B over 0 to 40 min; post-time 10 min; flow rate 1.0 mL/min; injection volume 20 μL ; monitored at wavelengths of 210, 254, 230, 280, and 360 nm. Mass spectrometry was carried out under positive ESI (electrospray ionization) using a Thermo Scientific LTQ Orbitrap Discovery instrument.

Experimental procedures for intermediates in Scheme 1.

4.1.1.1. 2-Methoxy-5,6,7,8-tetrahydronaphthalen-1-ol (1).^{61,68} To a well-stirred solution of 6-methoxy-1,2,3,4-tetrahydronaphthalene (14.15 g, 86.75 mmol) in *sec*-BuLi (100 mL, 110 mmol) at 0 °C, freshly distilled TMEDA (13.6 mL) was added dropwise. The reaction mixture was then stirred at room temperature for 1 h. The reaction mixture was cooled to 0 °C and B(OMe)₃ (12.5 mL, 110 mmol) was added dropwise. Then the reaction mixture was stirred for 1 h at room temperature. The reaction mixture was cooled to 0 °C, and glacial HOAc (7 mL) was added dropwise, followed by the dropwise addition of 35 wt.% H₂O₂ (15 mL). Finally, the reaction mixture was stirred at room temperature for 12 h. Saturated NH₄Cl (100 mL) was added, and product was extracted with Et₂O (3 x 400 mL). The combined organic phases were washed with brine and dried over Na₂SO₄, filtered, and concentrated *in vacuo*. Purification by flash column chromatography (silica gel, EtOAc/hexanes, gradient 2:98 to 5:95) yielded 2-methoxy-5,6,7,8-tetrahydronaphthalen-1-ol **1** (3.50 g, 19.6 mmol, 23% yield) as an off-white solid. ¹H NMR (CDCl₃, 300 MHz): δ 6.68 (1H, d, $J = 8.3$ Hz), 6.23 (1H, d, $J = 8.8$ Hz), 5.65 (1H, s), 3.84 (3H, s), 2.71 (4H, t, $J = 6.0$ Hz), 1.71 (4H, m).

4.1.1.2. 2-Methoxy-5,6,7,8-tetrahydronaphthalen-1-yl acetate (2).^{25,49,68} To a well-stirred solution of 2-methoxy-5,6,7,8-tetrahydronaphthalen-1-ol **1** (1.25 g, 7.01 mmol) dissolved in anhydrous CH₂Cl₂ (25 mL) was added Et₃N (1.5 mL, 10.8 mmol), Ac₂O (1.0 mL, 11 mmol), and DMAP (0.10 g, 0.9 mmol). The reaction mixture was stirred for 12 hours at room temperature. The solvents were removed *in vacuo*, and the crude product was subjected to flash chromatography (silica gel, 3:97 EtOAc/hexanes) to afford 2-methoxy-5,6,7,8-tetrahydronaphthalen-1-yl acetate **2** (1.50 g, 6.81 mmol, 95% yield) as a white solid. ¹H NMR (CDCl₃, 300 MHz): δ 6.91 (1H, d, $J = 8.4$ Hz), 6.75 (1H, d, $J = 8.4$ Hz), 3.78 (3H, s), 2.71 (2H, m), 2.54 (2H, m), 2.32 (3H, s), 1.74 (4H, m).

4.1.1.3. 2-Methoxy-5-oxo-5,6,7,8-tetrahydronaphthalen-1-yl acetate (3).^{25,49,68} A solution of DDQ (10.30 g, 22.70 mmol) in dioxane (40 mL) was added dropwise to a well stirred solution of 2-methoxy-5,6,7,8-tetrahydronaphthalen-1-yl acetate **2** (5.01 g, 23 mmol) in H₂O/dioxane (5/95) at rt. The reaction

mixture was stirred for 12 h, and the solid that precipitated was filtered and washed with EtOAc. The filtrates were evaporated under reduced pressure. To this was added saturated NaHCO₃ (100 mL), and the solution was extracted with Et₂O (3 x 200 mL). The combined organic phases were washed with brine, dried over Na₂SO₄, filtered and concentrated *in vacuo*. The crude product was subjected to flash column chromatography (silica gel, 30:70 EtOAc/hexanes) to afford 2-methoxy-5-oxo-5,6,7,8-tetrahydronaphthalen-1-yl acetate **3** (3.45 g, 14.7 mmol, 65% yield). ¹H NMR (CDCl₃, 300 MHz): δ 7.99 (1H, d, *J* = 8.7 Hz), 6.92 (1H, d, *J* = 8.7 Hz), 3.88 (3H, s), 2.79 (2H, t, *J* = 6.0 Hz), 2.60 (2H, m), 2.36 (3H, s), 2.10 (2H, p, *J* = 6.2 Hz).

4.1.1.4a. 5-Hydroxy-6-methoxy-3,4-dihydronaphthalen-1(2H)-one (4).^{25,49,68} Anhydrous K₂CO₃ (4.72 g, 34.1 mmol) was added to a well-stirred solution of 2-methoxy-5-oxo-5,6,7,8-tetrahydronaphthalen-1-yl acetate **3** (4.0 g, 17.1 mmol) in MeOH (100 mL) and H₂O (5 mL). The reaction mixture was stirred for 12 h at room temperature. The solvents were removed under reduced pressure followed by the addition of saturated NaHCO₃ (50 mL). The solution was extracted with CH₂Cl₂ (3 x 100 mL), and the combined organic phases were washed with brine, dried over Na₂SO₄ and filtered. The organic phases were evaporated *in vacuo* to afford 5-hydroxy-6-methoxy-3,4-dihydronaphthalen-1(2H)-one **4** (3.24 g, 16.9 mmol, 98% yield) as red crystals. ¹H NMR (CDCl₃, 300 MHz): δ 7.67 (1H, d, *J* = 8.6 Hz), 6.83 (1H, d, *J* = 8.6 Hz), 5.72 (1H, s), 3.96 (3H, s), 2.93 (2H, t, *J* = 6.0 Hz), 2.60 (2H, m), 2.10 (2H, p, *J* = 6.1 Hz).

4.1.1.5a. 5-((Tert-butyldimethylsilyl)oxy)-6-methoxy-3,4-dihydronaphthalen-1(2H)-one (5).^{25,49,68} Tetralone **4** (3.24 g, 16.9 mmol) was dissolved in anhydrous CH₂Cl₂ (75 mL) at room temperature. Et₃N (3.53 mL, 25.3 mmol) and DMAP (0.21 g, 1.69 mmol) were added, and the reaction mixture was stirred for 10 min. TBSCl (3.05 g, 20.2 mmol) was added in portions, and the reaction mixture was stirred for 12 h. The reaction was ended by the addition of H₂O (50 mL). The organic layers were separated, and the aqueous phases were extracted with CH₂Cl₂ (2 x 100 mL). The combined organic phases were washed with brine, dried over Na₂SO₄, filtered and evaporated to dryness under reduced pressure. Separation of the crude product by flash column chromatography (silica gel, 10:90 EtOAc/hexanes) afforded TBS-protected tetralone **5** (4.38 g, 14.3 mmol, 92% yield) as a colorless oil. ¹H NMR (CDCl₃, 300 MHz): δ 7.72 (1H, d, *J* = 8.6 Hz), 6.82 (1H, d, *J* = 8.6 Hz), 3.85 (3H, s), 2.90 (2H, t, *J* = 6.0 Hz), 2.57 (2H, m), 2.07 (2H, p, *J* = 6.1 Hz), 1.01 (9H, s), 0.18 (6H, s).

4.1.1.6. 5-((Tert-butyldimethylsilyl)oxy)-6-methoxy-1-(3,4,5-trimethoxyphenyl)-1,2,3,4-tetrahydronaphthalen-1-ol (6).^{49,68} To a well stirred solution of 3,4,5-trimethoxybromobenzene (7.57 g, 30.6 mmol) in anhydrous Et₂O (300 mL) at -78 °C, was added *n*-BuLi (20.8 mL, 24.5 mmol) dropwise. The reaction was stirred until the temperature reached -30 °C. The TBS-protected tetralone **5** (6.26 g, 20.4

mmol) dissolved in Et₂O (50 mL) was added dropwise to the reaction mixture, and the reaction mixture was stirred until it reached room temperature. H₂O (100 mL) was added, and the organic layer was separated. The aqueous phase was extracted with Et₂O (2 x 250 mL), and the combined organic phases were washed with brine. Removal of solvent under reduced pressure afforded crude product, which was subjected to flash column chromatography (silica gel, 20:80 EtOAc/hexanes) to afford tertiary alcohol **6** (6.86 g, 14.5 mmol, 69% yield) as a colorless oil. ¹H NMR (CDCl₃, 300 MHz): δ 6.67 (2H, m), 6.55 (2H, s), 3.89 (3H, s), 3.78 (9H, s), 2.89 (2H, m), 2.06 (2H, m), 1.60 (2H, m), 1.02 (9H, s), 0.23 (3H, s), 0.20 (3H, s).

4.1.1.7a. Tert-butyl((2-methoxy-5-(3,4,5-trimethoxyphenyl)-7,8-dihydronaphthalen-1-yl)oxy)dimethylsilane (7).^{49,68} A mixture of tertiary alcohol **6** (6.86 g, 14.1 mmol), glacial acetic acid (120 mL) and H₂O (400 mL) was refluxed for 12 h. The reaction was cooled and extracted with CH₂Cl₂ (2 x 300 mL). The combined organic phases were washed with brine, dried over Na₂SO₄ and filtered. Evaporation of the solvents under reduced pressure followed by drying under high vacuum afforded *tert*-butyl((2-methoxy-5-(3,4,5-trimethoxyphenyl)-7,8-dihydronaphthalen-1-yl)oxy)dimethylsilane **7** as a colorless oil (6.43 g, 14.1 mmol, quantitative yield). The crude product was carried on to the next step without further characterization.

4.1.1.8a. 2-Methoxy-5-(3,4,5-trimethoxyphenyl)-7,8-dihydronaphthalen-1-ol (8).^{49,68} The crude product **7** (6.43 g, 14.1 mmol) was dissolved in CH₂Cl₂ (150 mL) and cooled to 0 °C. To this was added TBAF (22 mL, 22 mmol) dropwise. The reaction was stirred for 10 min and ended by the addition of H₂O (100 mL). The organic layers were separated, and the aqueous phases were extracted with CH₂Cl₂ (2 x 300 mL). The combined organic phases were washed with brine and dried over Na₂SO₄. Filtration followed by evaporation of solvents afforded the crude product, which was separated by flash column chromatography (silica gel, 40:60 EtOAc/ hexanes) to afford **8** (4.50 g, 13.1 mmol, 97% yield) as an off-white solid. ¹H NMR (CDCl₃, 300 MHz): δ 6.62 (1H, d, *J* = 8.4 Hz), 6.58 (1H, d, *J* = 8.4 Hz), 6.56 (2H, s), 5.97 (1H, t, *J* = 4.6 Hz), 5.74 (1H, s), 3.89 (3H, s), 3.88 (3H, s), 3.84 (6H, s), 2.88 (2H, t, *J* = 8.2 Hz), 2.37 (2H, td, *J* = 8.2, 4.6 Hz). ¹³C NMR (CDCl₃, 75 MHz): δ 152.9, 145.8, 141.9, 139.0, 136.9, 128.9, 125.4, 122.3, 117.4, 107.2, 105.9, 60.9, 55.9, 22.8, 20.2. HPLC retention time – 14.00 min.

Experimental procedures for intermediates in Scheme 2.

4.1.1.9. 5-Bromo-6-methoxy-3,4-dihydronaphthalen-1(2H)-one (9).⁶⁰ 6-Methoxy-1-tetralone (1.06 g, 6.02 mmol) was stirred in 60 mL of H₂O. *N*-bromosuccinimide (1.07 g, 6.01 mmol) was added, and the reaction mixture was heated to 60 °C. H₂SO₄ (0.67 mL) was then added to the reaction mixture, which was heated for 5 h. The reaction mixture was extracted with EtOAc, and the organic layers were dried

over Na₂SO₄ and filtered. The solvent was then removed *in vacuo*, and the resulting solid was dissolved in methanol and recrystallized. The crystals were isolated by filtration and washed with cold methanol to afford the product **9** (1.22 g, 4.78 mmol, 81% yield) as a white solid. ¹H NMR (CDCl₃, 600 MHz): δ 8.09 (1H, d, *J* = 8.7 Hz), 6.91 (1H, d, *J* = 8.7 Hz), 4.00 (3H, s), 3.06 (2H, t, *J* = 6.2 Hz), 2.66 (2H, m), 2.15 (2H, p, *J* = 6.3 Hz). ¹³C NMR (CDCl₃, 151 MHz): δ 196.8, 159.8, 145.5, 128.4, 127.6, 113.0, 109.6, 56.5, 38.0, 30.5, 22.5. HRMS: Obsd 255.0016 [M + H⁺], Calcd for C₁₁H₁₂BrO₂⁺: 255.0015.

4.1.1.4b. 5-Hydroxy-6-methoxy-3,4-dihydronaphthalen-1(2H)-one (4).⁶¹ To a well-stirred solution of 5-bromo-6-methoxy-3,4-dihydronaphthalen-1(2H)-one **9** (0.50 g, 1.96 mmol) in THF at -78 °C, *n*-BuLi (4.90 mL, 7.84 mmol) was added dropwise. The reaction mixture was then stirred at -78 °C for 1 h and then allowed to warm to room temperature. B(OMe)₃ (0.45 mL, 3.92 mmol) was added dropwise, and the reaction mixture was stirred for 1 h at room temperature. Glacial acetic acid (0.22 mL) was added dropwise, followed by the addition of 35 wt.% H₂O₂ (0.48 mL) added dropwise. The reaction mixture was then stirred at room temperature for 12 h. Saturated NH₄Cl (20 mL) was added to the solution, and the mixture was extracted with EtOAc (3 x 50 mL). The combined organic phases were washed with brine and dried over Na₂SO₄, filtered, and concentrated *in vacuo*. Purification by flash column chromatography (silica gel, EtOAc/ hexanes) afforded the phenol **4** (0.32 g, 1.66 mmol, 85% yield) as a tan solid. ¹H NMR (CDCl₃, 600 MHz): δ 7.70 (1H, d, *J* = 8.6 Hz), 6.86 (1H, d, *J* = 8.6 Hz), 5.76 (1H, s), 3.98 (3H, s), 2.95 (2H, t, *J* = 6.2 Hz), 2.65 (2H, m), 2.13 (2H, p, *J* = 6.4 Hz). ¹³C NMR (CDCl₃, 151 MHz): δ 197.9, 149.9, 141.9, 130.4, 126.8, 120.0, 108.3, 56.1, 38.8, 22.9, 22.7. HRMS: Obsd 215.0679 [M + Na⁺], Calcd for C₁₁H₁₂NaO₃⁺: 215.0679.

4.1.1.5b. 5-((Tert-butyldimethylsilyl)oxy)-6-methoxy-3,4-dihydronaphthalen-1(2H)-one (5).⁴⁹ 5-hydroxy-6-methoxy-3,4-dihydronaphthalen-1(2H)-one **4** (1.05 g, 5.46 mmol) was stirred in 10 mL of CH₂Cl₂ at 0 °C. Triethylamine (0.84 mL, 6.03 mmol) and DMAP (0.27 g, 2.18 mmol) were then added. The reaction mixture was stirred for an additional 10 min before adding TBSCl (0.90 g, 5.97 mmol). The reaction was quenched with 100 mL of H₂O after 1 h. The reaction mixture was extracted with CH₂Cl₂ (3 x 100 mL), and the organic layer was dried over Na₂SO₄. The organic layer was then filtered, and the solvent was removed *in vacuo*. The crude mixture was purified by flash chromatography (silica gel, EtOAc/ hexanes) to afford silyl ether **5** (1.58 g, 5.16 mmol, 95% yield) as an orange oil. ¹H NMR (CDCl₃, 600 MHz): δ 7.54 (1H, d, *J* = 8.6 Hz), 6.64 (1H, d, *J* = 8.7 Hz), 3.67 (3H, s), 2.72 (2H, t, *J* = 6.1 Hz), 2.42 (2H, m), 1.89 (2H, p, *J* = 6.4 Hz), 0.83 (9H, s), 0.00 (6H, s). ¹³C NMR (CDCl₃, 151 MHz): δ 198.0, 154.0, 141.3, 136.1, 126.8, 121.5, 109.2, 54.9, 38.7, 26.1, 24.4, 22.9, 18.9, -3.8. HRMS: Obsd 307.1727 [M + H⁺], Calcd for C₁₇H₂₇O₃Si⁺: 307.1724.

4.1.1.7b. *Tert*-butyl((2-methoxy-5-(3,4,5-trimethoxyphenyl)-7,8-dihydronaphthalen-1-yl)oxy)dimethylsilane (**7**).^{25,62} To a solution of 3,4,5-trimethoxybromobenzene (1.62 g, 6.55 mmol) in anhydrous THF (20 mL), *n*-BuLi (2.62 mL, 6.55 mmol) was added dropwise at -78 °C. The reaction mixture was stirred for 30 min at -78 °C. A solution of 5-((*tert*-butyldimethylsilyl)oxy)-6-methoxy-3,4-dihydronaphthalen-1(*2H*)-one **5** (1.00 g, 3.27 mmol) in THF (10 mL) was added dropwise, and the reaction mixture was then allowed warm to 0 °C over 3 h. The reaction was then cooled to -78 °C, and triethylamine (3.68 mL, 26.16 mmol) and MsCl (1.01 mL, 13.08 mmol) were added dropwise to the solution. The reaction mixture was allowed to warm to room temperature over a period of 8 h. The reaction mixture was quenched with H₂O (100 mL), and the reaction mixture was then extracted with EtOAc (3 x 100 mL). The combined organic phases were washed with brine, dried over Na₂SO₄, filtered, and the solvent was removed *in vacuo*. The resulting crude product was then subjected to flash column chromatography (silica gel, EtOAc/ hexanes) to afford *tert*-butyl((2-methoxy-5-(3,4,5-trimethoxyphenyl)-7,8-dihydronaphthalen-1-yl)oxy)dimethylsilane **7** (0.82 g, 1.80 mmol, 55% yield). ¹H NMR (CDCl₃, 600 MHz): δ 6.44 (1H, d, *J* = 8.4 Hz), 6.40 (1H, d, *J* = 8.5 Hz), 6.37 (2H, s), 5.75 (1H, t, *J* = 4.6 Hz), 3.69 (3H, s), 3.65 (6H, s), 3.58 (3H, s), 2.69-2.64 (2H, m), 2.13 (2H, td, *J* = 7.9, 4.7 Hz), 0.83 (9H, s), 0.00 (6H, s). ¹³C NMR (CDCl₃, 151 MHz): δ 152.9, 149.7, 141.4, 139.8, 137.0, 137.0, 128.7, 128.1, 124.9, 118.9, 108.1, 106.0, 60.9, 56.1, 26.1, 23.1, 21.7, 18.9, -3.9.

4.1.1.8b. **2-Methoxy-5-(3,4,5-trimethoxyphenyl)-7,8-dihydronaphthalen-1-ol (8)**.⁴⁹ *Tert*-butyl((2-methoxy-5-(3,4,5-trimethoxyphenyl)-7,8-dihydronaphthalen-1-yl)oxy)dimethylsilane **7** (0.82 g, 1.80 mmol) was dissolved in THF and cooled to 0 °C. TBAF (0.71 g, 2.70 mmol) was added to the solution. The reaction mixture was stirred 30 min and then quenched with 50 mL of H₂O. The aqueous layer was extracted with EtOAc (3 x 100 mL), and the organic layer was dried over Na₂SO₄. The organic layer was then filtered, and the solvent was removed *in vacuo*. Purification by flash chromatography (silica gel, EtOAc/ hexanes) afforded 2-methoxy-5-(3,4,5-trimethoxyphenyl)-7,8-dihydronaphthalen-1-ol **8** (0.62 g, 1.80 mmol, quantitative yield) as a white solid. ¹H NMR (CDCl₃, 600 MHz): δ 6.65 (1H, d, *J* = 8.4 Hz), 6.61 (1H, d, *J* = 8.4 Hz), 6.58 (2H, s), 5.99 (1H, t, *J* = 4.7 Hz), 5.74 (1H, s), 3.91 (6H, s), 3.86 (6H, s), 2.93 (2H, t, *J* = 8.4 Hz), 2.40 (2H, td, *J* = 8.0, 4.7 Hz). ¹³C NMR (CDCl₃, 151 MHz): δ 152.9, 145.8, 142.0, 139.5, 136.9, 129.0, 125.4, 122.3, 117.4, 107.2, 105.8, 61.0, 56.1, 56.0, 22.8, 20.2. HRMS: Obsd 343.1541 [M + H⁺], Calcd for C₂₀H₂₃O₅⁺: 343.1540. HPLC retention time 7.47 min.

Experimental procedures for intermediates in Scheme 3.

4.1.1.10. *N*'-(5-((*tert*-butyldimethylsilyl)oxy)-6-methoxy-3,4-dihydronaphthalen-1(*2H*)-ylidene)-4-methylbenzenesulfonohydrazide (**10**).⁴⁹ To a well-stirred solution of tetralone **5** (6.20 g, 13.1 mmol) in

anhydrous EtOH (120 mL) was added *p*-toluenesulfonylhydrazide (3.77 g, 20.3 mmol). Solution was achieved within 5 min, at which point *p*-TSA monohydrate (0.17 g, 1.01 mmol) was added, and the reaction mixture was stirred at room temperature for 12 h. Hydrazone **10** precipitated as a white solid, which was then filtered, washed with ice-cold EtOH, and dried under reduced pressure to afford **10** (5.20 g, 11.0 mmol, 54% yield) as a white solid. ¹H NMR (CDCl₃, 500 MHz): δ 7.93 (2H, d, *J* = 8.3 Hz), 7.86 (1H, s), 7.61 (1H, d, *J* = 8.7 Hz), 7.31 (2H, d, *J* = 8.0 Hz), 6.73 (1H, d, *J* = 8.8 Hz), 3.79 (3H, s), 2.71-2.65 (2H, m), 2.42 (2H, t, *J* = 6.6 Hz), 2.40 (3H, s), 1.80 (2H, p, *J* = 6.6 Hz), 0.97 (9H, s), 0.13 (6H, s).

4.1.1.11. (5-((*Tert*-butyldimethylsilyloxy)-6-methoxy-3,4-dihydronaphthalen-1-yl)(3,4,5-trimethoxyphenyl)methanol (11).⁴⁹ *n*-BuLi (13.5 mL, 33.8 mmol) was added to freshly distilled TMEDA (30 mL), and the mixture was cooled to -50 °C. At this point, hydrazine **10** (4.00 g, 8.44 mmol) was added, and the reaction mixture was stirred until the temperature reached 25 °C. To the reaction mixture 3,4,5-trimethoxybenzaldehyde (6.62 g, 33.8 mmol) was added, and the reaction was stirred for 1 h. H₂O (25 mL) was added, and the product was extracted with EtOAc (2 x 100 mL). The combined organic phases were washed with 10% aqueous CuSO₄ solution (100 mL) and brine, dried over Na₂SO₃, filtered, and evaporated under reduced pressure. Purification of the crude product by flash column chromatography (silica gel, 16:84 EtOAc/hexanes) yielded alcohol **11** (2.22 g, 4.56 mmol, 54% yield) as a pale-yellow oil. The resulting secondary alcohol was carried on to the next step without characterization.

4.1.1.12a. (5-((*Tert*-butyldimethylsilyloxy)-6-methoxy-3,4-dihydronaphthalen-1-yl)(3,4,5-trimethoxyphenyl)methanone (12).⁴⁹ To a well-stirred solution of Dess-Martin periodinane (1.30 g, 2.24 mmol) in dry CH₂Cl₂ (20 mL) at room temperature was added a solution of alcohol **11** (1.00 g, 2.04 mmol) in anhydrous CH₂Cl₂ (20 mL) followed by 10% aqueous Na₂S₂O₄ (0.05 mL). After stirring for 5 min, a solution of 10% aqueous Na₂S₂O₃ and saturated NaHCO₃ (30 mL, 1:1 ratio) was added, and the reaction mixture was stirred for 5 min. The product was extracted into CH₂Cl₂ (3 x 50 mL). The combined organic phases were filtered, and the solvent was removed under reduced pressure. The crude product was purified by flash column chromatography (silica gel, 10:90 EtOAc/hexanes) to afford ketone **12** (0.68 g, 1.41 mmol, 69% yield) as a pale-yellow oil. ¹H NMR (CDCl₃, 500 MHz): δ 7.14 (2H, s), 6.80 (1H, d, *J* = 8.4 Hz), 6.63 (1H, d, *J* = 8.5 Hz), 6.32 (1H, t, *J* = 4.7 Hz), 3.91 (3H, s), 3.84 (6H, s), 3.77 (3H, s), 2.88 (2H, t, *J* = 8.0 Hz), 2.43 (2H, td, *J* = 7.9, 4.8 Hz), 1.01 (9H, s), 0.17 (6H, s).

4.1.1.13a. (5-Hydroxy-6-methoxy-3,4-dihydronaphthalen-1-yl)(3,4,5-trimethoxyphenyl)methanone (13).⁴⁹ Ketone **12** (0.68 g, 1.41 mmol) was dissolved in CH₂Cl₂ (25 mL), and the reaction mixture was cooled to 0 °C. To this was added TBAF (2.82 mL, 2.82 mmol) dropwise. The reaction mixture was

stirred for 10 min and terminated by the addition of H₂O (25 mL). The organic layers were separated, and the aqueous phases were extracted with CH₂Cl₂ (2 x 25 mL). The combined organic phases were washed with brine and dried over Na₂SO₄. Filtration followed by evaporation of solvents afforded the crude product, which was separated by flash column chromatography (silica gel, 40:60 EtOAc/ hexanes) to afford **13** (0.29 g, 0.78 mmol, 55% yield) as an off-white solid. ¹H NMR (CDCl₃, 500 MHz): δ 7.16 (2H, s), 6.77 (1H, d, *J* = 8.4 Hz), 6.65 (1H, d, *J* = 8.4 Hz), 6.33 (1H, t, *J* = 4.7 Hz), 5.74 (1H, s), 3.92 (3H, s), 3.88 (3H, s), 3.85 (6H, s), 2.91 (2H, t, *J* = 8.0 Hz), 2.47 (2H, td, *J* = 8.0, 4.7 Hz). ¹³C NMR (CDCl₃, 151 MHz): δ 196.3, 152.8, 146.4, 142.4, 142.2, 138.3, 133.0, 133.0, 125.9, 121.4, 117.5, 107.8, 107.5, 60.9, 56.2, 55.9, 22.5, 19.8. HRMS: Obsd 371.1489 [M + H⁺], Calcd for C₂₁H₂₃O₆⁺ 371.1489.

Experimental procedures for intermediates in Scheme 4.

4.1.1.14. ((5-Bromo-2-methoxy-7,8-dihydronaphthalen-1-yl)oxy)(*tert*-butyl)dimethylsilane (14**).**⁶³ To a solution of 5-((*tert*-butyldimethylsilyl)oxy)-6-methoxy-3,4-dihydronaphthalen-1(2*H*)-one **5** (0.66 g, 2.17 mmol) in toluene (50 mL) phosphorus tribromide (3.25 mL, 1 M in dichloromethane) was added. The reaction mixture was heated to 80 °C for 3 h. Water was added, and the mixture was extracted with EtOAc (3 x 50 mL). The organic layer was dried over Na₂SO₄, filtered, concentrated under reduced pressure, and purified by flash chromatography (silica gel, EtOAc/ hexanes) to afford vinyl bromide **14** (0.51 g, 1.4 mmol, 63% yield) as an orange oil. ¹H NMR (CDCl₃, 500 MHz): δ 7.16 (1H, d, *J* = 8.5 Hz), 6.69 (1H, d, *J* = 8.5 Hz), 6.29 (1H, t, *J* = 4.8 Hz), 3.80 (3H, s), 2.86-2.82 (2H, m), 2.29 (2H, td, *J* = 8.0, 4.9 Hz), 1.00 (9H, s), 0.16 (6H, s). ¹³C NMR (CDCl₃, 151 MHz): δ 150.6, 141.1, 128.7, 127.7, 126.7, 121.1, 120.1, 108.2, 54.9, 26.1, 26.0, 25.0, 21.5, -4.0.

4.1.1.12b. (5-((*Tert*-butyldimethylsilyl)oxy)-6-methoxy-3,4-dihydronaphthalen-1-yl)(3,4,5-trimethoxyphenyl)methanone (12**).** To a solution of vinyl bromide **14** (0.51 g, 1.4 mmol) in THF (50 mL) at -78 °C, *n*-BuLi (0.56 mL, 2.5 M in hexanes) was added. The reaction mixture was stirred for 15 min, then *N*,3,4,5-tetramethoxy-*N*-methylbenzamide dissolved in THF was added. The reaction was allowed to warm to room temperature over a period of 8 h. Upon completion, water was added, and the mixture was extracted with EtOAc (3 x 50 mL). The organic layer was dried over Na₂SO₄, filtered, concentrated under reduced pressure, and purified by flash chromatography (silica gel, EtOAc/hexanes) to afford dihydronaphthalene analog **12** (0.32 g, 0.66 mmol, 47% yield) as a clear oil. ¹H NMR (CDCl₃, 500 MHz): δ 7.14 (2H, s), 6.80 (1H, d, *J* = 8.4 Hz), 6.63 (1H, d, *J* = 8.5 Hz), 6.32 (1H, t, *J* = 4.7 Hz), 3.91 (3H, s), 3.84 (6H, s), 3.77 (3H, s), 2.88 (2H, t, *J* = 8.0 Hz), 2.43 (2H, td, *J* = 7.9, 4.8 Hz), 1.01 (9H, s), 0.17 (6H, s). ¹³C NMR (CDCl₃, 126 MHz): δ 196.4, 152.8, 150.2, 142.3, 141.5, 138.6, 133.1, 133.0, 127.3, 125.8, 119.2, 108.7, 107.4, 60.9, 56.2, 54.8, 26.0, 22.8, 21.3, 18.8, -4.0.

4.1.1.13b. (5-Hydroxy-6-methoxy-3,4-dihydronaphthalen-1-yl)(3,4,5-trimethoxyphenyl)methanone (13). To a solution of silyl ether **12** (0.32 g, 0.66 mmol) in THF concentrated HCl (5 mL) was added. The reaction was stirred at room temperature for 3 h. Upon completion, saturated aqueous NaHCO₃ was added, and the mixture was extracted with EtOAc (3 x 50 mL). The organic layer was dried over Na₂SO₄, filtered, concentrated under reduced pressure, and purified by flash chromatography (silica gel, EtOAc/hexanes) to afford **13** (0.24 g, 0.66 mmol, quantitative yield) as a white solid. To prevent the dihydronaphthalene ring from aromatizing the reaction mixture was not heated above room temperature during the deprotection reaction or during the purification process. ¹H NMR (CDCl₃, 500 MHz): δ 7.16 (2H, s), 6.77 (1H, d, *J* = 8.4 Hz), 6.65 (1H, d, *J* = 8.4 Hz), 6.33 (1H, t, *J* = 4.7 Hz), 5.74 (1H, s), 3.92 (3H, s), 3.88 (3H, s), 3.85 (6H, s), 2.91 (2H, t, *J* = 8.0 Hz), 2.47 (2H, td, *J* = 8.0, 4.7 Hz). ¹³C NMR (CDCl₃, 151 MHz): δ 196.3, 152.8, 146.4, 142.4, 142.2, 138.3, 133.0, 133.0, 125.9, 121.4, 117.5, 107.8, 107.5, 60.9, 56.2, 55.9, 22.5, 19.8. HRMS: Obsd 371.1489 [M + H⁺], Calcd for C₂₁H₂₃O₆⁺ 371.1489. HPLC retention time – 5.18 min.

Experimental procedures for intermediates in Scheme 5.

4.1.1.15. Dibenzyl (2-methoxy-5-(3,4,5-trimethoxyphenyl)-7,8-dihydronaphthalen-1-yl) phosphate (15).^{47,49} To a well-stirred solution of **13** (1.40 g, 4.09 mmol) in CH₃CN (25 mL) at -25 °C, CCl₄ (25 mL) was added, and the reaction mixture was stirred for approximately 15 min. DIPEA (1.51 mL, 8.61 mmol) and DMAP (0.05 g, 0.41 mmol) were added, followed by the addition of dibenzyl phosphonate (1.36 mL, 6.14 mmol), and the reaction mixture was stirred for approximately 2 h. The reaction was quenched with a 0.5 M KH₂PO₄ solution (30 mL). The solution was extracted with EtOAc (3 x 100 mL). The combined organic phases were washed with brine, dried over Na₂SO₄, filtered and concentrated *in vacuo*. Purification by flash column chromatography (silica gel, 40:60 EtOAc/hexanes) afforded dibenzyl-KGP03-phosphate **15** (2.16 g, 3.58 mmol, 88% yield) as a yellow oil. The resulting dibenzyl ester was carried on to the next step without characterization.

4.1.1.16. Disodium 2-methoxy-5-(3,4,5-trimethoxyphenyl)-7,8-dihydronaphthalen-1-yl phosphate (16).^{47,49} To a solution of dibenzyl-KGP03-phosphate **15** (2.16 g, 3.58 mmol) in acetonitrile (60 mL), sodium iodide (1.07 g, 7.16 mmol) was added. Before dropwise addition of chlorotrimethylsilane (0.91 mL, 7.16 mmol), the mixture was stirred for 2 min, and approximately 30 min later the reaction was terminated with 1% aqueous sodium thiosulfate (1 mL). Removal of the acetonitrile *in vacuo* afforded a crude mixture, which was dissolved in water-dichloromethane and washed with water (4 x 60 mL). Concentration (facilitated by toluene azeotrope) of the aqueous layer resulted in isolation of the crude phosphoric acid intermediate, which was subjected to drying under vacuum for approximately 1 h, and

then dissolved in dry methanol (30 mL). Next, sodium methoxide (0.39 g, 7.16 mmol) was added. The mixture was stirred 6 h and additional methanol was added to effect dissolution. After filtration of the solution, concentration of the methanol *in vacuo* led to an off-white solid, which was reprecipitated from water-ethanol to yield **16** (1.10 g, 2.36 mmol, 66% yield). ¹H NMR (D₂O, 300 MHz): δ 6.67 (1H, d, *J* = 8.4 Hz), 6.65 (2H, s), 6.64 (1H, d, *J* = 8.4 Hz), 5.98 (1H, t, *J* = 4.6 Hz), 3.75 (6H, s), 3.74 (6H, s), 2.86 (2H, t, *J* = 8.2 Hz), 2.23 (2H, td, *J* = 8.2, 4.6 Hz). ¹³C NMR (D₂O, 75 MHz): δ 152.2, 151.6, 140.0, 140.0, 138.5, 137.8, 135.8, 131.5, 131.5, 128.2, 128.1, 126.7, 120.7, 109.1, 106.3, 61.0, 56.0, 55.5, 22.5, 21.8. HPLC retention time 3.07 min.

4.1.1.17. Dibenzyl (2-methoxy-5-(3,4,5-trimethoxybenzoyl)-7,8-dihydronaphthalen-1-yl) phosphate (17).^{47,49} To a well-stirred solution of **13** (0.74 g, 2.00 mmol) in CH₃CN (15 mL) at -25 °C CCl₄ (15 mL) was added, and the reaction mixture was stirred for approximately 15 min. DIPEA (0.51 mL, 2.91 mmol) and DMAP (0.02 g, 0.16 mmol) were added, followed by the addition of dibenzyl phosphonate (0.53 mL, 2.40 mmol), and the reaction mixture was stirred for approximately 2 h. The reaction was quenched with a 0.5 M KH₂PO₄ solution (30 mL). The solution was extracted with EtOAc (3 x 100 mL). The combined organic phases were washed with brine, dried over Na₂SO₄, filtered and concentrated *in vacuo*. Purification by flash column chromatography (silica gel, 40:60 EtOAc/hexanes) afforded dibenzyl-KGP413-phosphate **17** (0.67 g, 1.06 mmol, 84% yield) as a yellow oil. The resulting dibenzyl ester was carried on to the next step without characterization.

4.1.1.18. Disodium 2-methoxy-5-(3,4,5-trimethoxybenzoyl)-7,8-dihydronaphthalen-1-yl phosphate (18).^{47,49} To a solution of dibenzyl-KGP413-phosphate **17** (0.67 g, 1.06 mmol) in acetonitrile (20 mL), sodium iodide (0.32 g, 2.12 mmol) was added. Before dropwise addition of chlorotrimethylsilane (0.27 mL, 2.12 mmol), the mixture was stirred for 2 min, and approximately 30 min later the reaction was terminated with 1% aqueous sodium thiosulfate (1 mL). Removal of the acetonitrile *in vacuo* afforded a crude mixture, which was dissolved in water-dichloromethane and washed with water (4 x 20 mL). Concentration (facilitated by toluene azeotrope) of the aqueous layer resulted in isolation of the crude phosphoric acid intermediate, which was subjected to drying under vacuum for approximately 1 h, and then dissolved in dry methanol (10 mL). Next, sodium methoxide (0.12 g, 2.12 mmol) was added. The mixture was stirred 6 h, and additional methanol was added to effect dissolution. After filtration of the solution, concentration of the methanol *in vacuo* led to an off-white solid, which was reprecipitated from water-ethanol to yield **18** (0.22 g, 0.45 mmol, 42% yield). ¹H NMR (D₂O, 300 MHz): δ 7.11 (2H, s), 6.77 (1H, d, *J* = 8.4 Hz), 6.69 (1H, d, *J* = 8.4 Hz), 6.44 (1H, t, *J* = 4.7), 3.75 (6H, s), 3.75 (3H, s), 3.70 (3H, s), 2.86 (2H, t, *J* = 8.0 Hz), 2.34 (2H, td, *J* = 8.0, 4.7 Hz). ¹³C NMR (D₂O, 75 MHz): δ 200.1, 152.3, 152.2, 152.1, 141.5, 140.1, 139.0, 137.3, 133.5, 130.8, 130.8, 124.9, 120.9, 109.5, 108.5, 107.9, 61.0, 56.1, 55.4,

22.6, 21.0. ^{31}P NMR (D_2O , 122 MHz): δ 0.92, 0.79. HRMS: Obsd 495.0791 [$\text{M} + \text{H}^+$], Calcd for $\text{C}_{21}\text{H}_{22}\text{Na}_2\text{O}_9\text{P}^+$ 495.0791. HPLC retention time 8.05 min.

4.2. Biological evaluation

4.2.1. Cell lines and Sulforhodamine B (SRB) assay.

Inhibition of growth of human cancer cells was assessed using the sulforhodamine B assay (SRB), as previously described.^{69–71} Cancer cell lines (DU-145, SK-OV-3, and NCI-H460) (obtained from ATCC) were plated at 7000–8000 cells/well into 96-well plates using DMEM supplemented with 5% fetal bovine serum / 1% gentamicin sulfate and incubated for 24 h at 37 °C in a humidified incubator in a 5% CO_2 atmosphere. Compounds to be tested were dissolved in DMSO to generate a 10 mg/mL stock solution. Serial dilutions were made and added to the plates. Doxorubicin and paclitaxel were used as positive controls. After a 48 h treatment, the cells were fixed with trichloroacetic acid (10% final concentration), washed, dried, stained with SRB dye, washed to remove excess dye, and dried. SRB dye was solubilized, and absorbances were measured at wavelength 540 nm and normalized to values at wavelength 630 nm using an automated Biotek plate reader. A growth inhibition of 50% (GI_{50} or the drug concentration causing 50% reduction in the net protein increase) was calculated from the absorbance data.

4.2.2. Colchicine binding assay.⁷²

Inhibition of [^3H]colchicine binding to tubulin was measured using 100 μL reaction mixtures containing 1.0 μM tubulin, 5.0 μM [^3H]colchicine (from Perkin-Elmer), 5% (v/v) dimethyl sulfoxide, potential inhibitors at 1.0 or 5.0 μM , as indicated, and components that stabilize the colchicine binding activity of tubulin (1.0 M monosodium glutamate [adjusted to pH 6.6 with HCl in a 2.0 M stock solution], 0.5 mg/mL bovine serum albumin, 0.1 M glucose-1-phosphate, 1.0 mM MgCl_2 , and 1.0 mM GTP). Incubation was for 10 min at 37 °C, when the binding reaction in control reaction mixtures is 40–60% complete. Reactions were stopped with 2.0 mL of ice-cold water, and the reaction mixtures were placed on ice. Each sample was poured onto a stack of two DEAE-cellulose filters (from Whatman), followed by 6 mL of ice-cold water. The samples were aspirated under reduced vacuum. The filters were washed three times with 2 mL water and placed into vials containing 5 mL of Biosafe II scintillation cocktail. Samples were counted 18 h later in a Beckman scintillation counter. Samples with inhibitors were compared to samples with no inhibitor, and percent inhibition was determined. All samples were corrected for the amount of radiolabel bound to the filters in the absence of tubulin.

4.2.3. Inhibition of tubulin polymerization.⁴³

Tubulin polymerization experiments were performed in 0.25 mL reaction mixtures (final volume) that contained 1 mg/mL (10 μ M) purified bovine brain tubulin, 0.8 M monosodium glutamate (pH 6.6), 4% (v/v) dimethyl sulfoxide, 0.4 mM GTP, and different compound concentrations. All reaction components except GTP were preincubated for 15 min at 30 °C in 0.24 mL. The mixtures were cooled to 0 °C, and 10 μ L of 10 mM GTP was added. Reaction mixtures were transferred to cuvettes held at 0 °C in Beckman DU-7400 and DU-7500 spectrophotometers equipped with electronic temperature controllers. The temperature was jumped to 30 °C, taking about 30 s, and polymerization was followed at 350 nm for 20 min. The IC₅₀ was defined as the compound concentration that inhibited extent of polymerization by 50% after 20 min.

4.2.4. *In vivo* color Doppler ultrasound imaging with KGP04.

A549 human lung cancer cells (3x10⁶, in 200 μ L serum free medium with 50% Matrigel[®]; cell line provided by Professor John Minna (UT Southwestern)) were implanted subcutaneously in the right hind thigh of anesthetized nude rats (8-10 week old female; T-cell-deficient, athymic homozygous nude rat; Charles River, NCI at Frederick, Frederick, MD).⁷³ The tumor was allowed to grow until it reached about 9 mm diameter. At this time the rat was anesthetized with isoflurane and color-Doppler ultrasound was performed using a Vevo 2100 [Fuji (VisualSonics), Toronto, Canada] before and 2 h after administration of KGP04 IP (15 mg/kg dissolved in 500 μ L saline) *in situ*.¹⁴ All animal procedures were approved by the University of Texas Southwestern Medical Center Institutional Animal Care and Use Committee under APN101222 and 102169.

4.2.5. *In vivo* bioluminescence imaging (BLI) with KGP152.¹⁷

MDA-MB-231-luc cells (1x10⁶ in 100 μ L of PBS with 50% Matrigel[®]; original cell line from ATCC, with transfected cell line recently provided by Dr. Edward Graves, Stanford University) were injected directly into the left upper mammary fat pad of three anesthetized BALB/c SCID mice. Tumors were allowed to grow over about 3 months and then BLI was performed using an IVIS[®] Spectrum system (Perkin-Elmer (Xenogen), Alameda, CA). *D*-luciferin (128 mg/kg in PBS in a total volume of 80 μ L; Gold Biotechnology Inc., St. Louis, MO) was administered subcutaneously (SC) in the foreback neck region. Immediately after luciferin injection, a series of BLI images was acquired over a period of 30 min using auto exposure time.¹⁷ Following baseline BLI, mice were injected intraperitoneally (IP) respectively with 100, 150, and 200 mg/kg KGP152 in saline. Dynamic BLI was repeated 4 and 24 h post-treatment with administration of fresh luciferin on each occasion. All animal procedures were approved by the University of Texas Southwestern Medical Center Institutional Animal Care and Use Committee under APN101222 and 102169.

Supplementary data:

Electronic supplementary information (ESI) available: Supplementary data including (^1H NMR, ^{13}C NMR, ^{31}P NMR, HRMS, HPLC) for targets compounds and intermediates (^1H NMR, ^{13}C NMR, only), phosphatase enzyme cleavage data, and X-ray crystallography (CCDC 1018601 and 1842517) for **KGP03** and **KGP413** associated with this article can be found in the online supplementary data file.

Conflicts of Interest:

A significant portion of the work presented in this manuscript was funded through Mateon Therapeutics, Inc. (formerly OXiGENE Inc.), and this relationship is properly indicated in the acknowledgement section. Dr. David Chaplin is a former employee and current member of the Board of Directors of Mateon Therapeutics, Inc. He is included as a co-author on this manuscript for his valuable contributions to the overall project. In addition, one of the authors (KGP) is a former paid consultant with Mateon Therapeutics, Inc. and current shareholder. We are pleased with this productive and useful long-term scientific collaboration and funding relationship with Mateon Therapeutics, Inc., and it is important to note that there is absolutely no actual conflict of interest associated with the science presented in this manuscript.

Acknowledgements:

The research was supported in part by the National Cancer Institute of the National Institutes of Health (Grant No. 5R01CA140674 to K.G.P, M.L.T, and R.P.M), the Cancer Prevention and Research Institute of Texas (CPRIT, Grant No. RP140399 to K.G.P., M.L.T., and R.P.M., Grant No. RP170696 to K.G.P., M.L.T., and MIRA RP120670-P3 to RPM), and Mateon Therapeutics, Inc. (grant to K.G.P. and M.L.T.) for their financial support of this project. The content is solely the responsibility of the authors and does not necessarily reflect the official views of the National Institutes of Health. The authors also thank Dr. Craig Moehnke and Dr. Michelle Nemec (Director) for the use of the shared Molecular Biosciences Center at Baylor University, Dr. Alejandro Ramirez (Mass Spectrometry Core Facility, Baylor University), Dr. Christine A. Herdman (help with spectral characterization), and Dr. Kevin Klausmeyer (X-ray analysis). Imaging was facilitated with the assistance of the Southwestern Small Animal Imaging Resource (SW-SAIRP), which is supported in part by NCI U24 CA126608, the Harold C. Simmons Cancer Center through an NCI Cancer Center Support Grant, 1P30CA142543, and the Department of Radiology. The IVIS Spectrum was acquired with the assistance of NIH Shared Instrumentation Grant S10RR024757. We are grateful to Professor J. Hill (Cardiology, UTSW) for providing access to the Vevo 2100, which was acquired under the NIH Shared Instrumentation Grant S10 RR031859.

References and notes

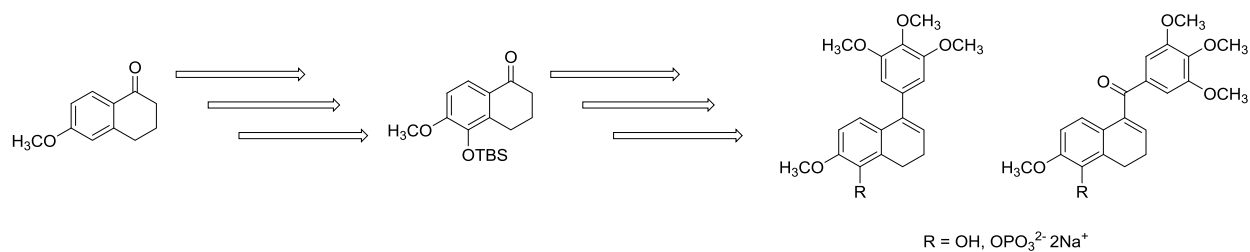
1. R. J. Ludford, *JNCI J. Natl. Cancer Inst.*, 1945, **6**, 89–101.
2. G. R. Pettit, S. B. Singh, E. Hamel, C. M. Lin, D. S. Alberts and D. Garcia-Kendal, *Experientia*, 1989, **45**, 209–211.
3. G. R. Pettit, S. B. Singh, M. L. Niven, E. Hamel and J. M. Schmidt, *J. Nat. Prod.*, 1987, **50**, 119–131.
4. G. R. Pettit, S. B. Singh, M. R. Boyd, E. Hamel, R. K. Pettit, J. M. Schmidt and F. Hogan, *J. Med. Chem.*, 1995, **38**, 1666–1672.
5. K. Pinney, G. Pettit, M. Trawick, C. Jelinek and D. Chaplin, in *Anticancer Agents from Natural Products, Second Edition*, CRC Press, 2011, pp. 27–64.
6. J. Griggs, J. C. Metcalfe and R. Hesketh, *Lancet Oncol.*, 2001, **2**, 82–87.
7. S. N. A. Bukhari, G. B. Kumar, H. M. Revankar and H.-L. Qin, *Bioorganic Chem.*, 2017, **72**, 130–147.
8. H. P. Hsieh, J. P. Liou and N. Mahindroo, *Curr. Pharm. Des.*, 2005, **11**, 1655–1677.
9. H. Rajak, P. K. Dewangan, V. Patel, D. K. Jain, A. Singh, R. Veerasamy, P. C. Sharma and A. Dixit, *Curr. Pharm. Des.*, 2013, **19**, 1923–1955.
10. G. C. Tron, T. Pirali, G. Sorba, F. Pagliai, S. Busacca and A. A. Genazzani, *J. Med. Chem.*, 2006, **49**, 3033–3044.
11. K. G. Pinney, K. E. Carlson and J. A. Katzenellenbogen, *Steroids*, 1992, **57**, 222–232.
12. K. G. Pinney, F. Wang, M. Hadimani, M. Mejia, US20070082872 A1, 2007.
13. K. G. Pinney, A. D. Bounds, K. M. Dingeman, V. P. Mocharla, G. R. Pettit, R. Bai and E. Hamel, *Bioorg. Med. Chem. Lett.*, 1999, **9**, 1081–1086.
14. M. B. Hadimani, M. T. MacDonough, A. Ghatak, T. E. Strecker, R. Lopez, M. Sriram, B. L. Nguyen, J. J. Hall, R. J. Kessler, A. R. Shirali, L. Liu, C. M. Garner, G. R. Pettit, E. Hamel, D. J. Chaplin, R. P. Mason, M. L. Trawick and K. G. Pinney, *J. Nat. Prod.*, 2013, **76**, 1668–1678.
15. M. T. MacDonough, Z. Shi and K. G. Pinney, *Tetrahedron Lett.*, 2015, **56**, 3624–3629.
16. T. E. Strecker, S. O. Odutola, R. Lopez, M. S. Cooper, J. K. Tidmore, A. K. Charlton-Sevcik, L. Li, M. T. MacDonough, M. B. Hadimani, A. Ghatak, L. Liu, D. J. Chaplin, R. P. Mason, K. G. Pinney and M. L. Trawick, *Cancer Lett.*, 2015, **369**, 229–241.

17. H. Zhou, R. R. Hallac, R. Lopez, R. Denney, M. T. MacDonough, L. Li, L. Liu, E. E. Graves, M. L. Trawick, K. G. Pinney and R. P. Mason, *Am. J. Nucl. Med. Mol. Imaging*, 2015, **5**, 143–153.
18. M. B. Hadimani, R. J. Kessler, J. A. Kautz, A. Ghatak, A. R. Shirali, H. O'Dell, C. M. Garner and K. G. Pinney, *Acta Crystallogr. C*, 2002, **58**, o330-332.
19. R. J. Kessler, "Synthesis and Evaluation of New Inhibitors of Tubulin Polymerization and Their Corresponding Prodrugs as Potential Vascular Targeting Agents." Master's Thesis, Baylor University, 2002.
20. A. Shirali, M. Sriram, J. J. Hall, B. L. Nguyen, R. Guddneppanavar, M. B. Hadimani, J. F. Ackley, R. Siles, C. J. Jelinek, P. Arthasery, R. C. Brown, V. L. Murrell, A. McMordie, S. Sharma, D. J. Chaplin and K. G. Pinney, *J. Nat. Prod.*, 2009, **72**, 414–421.
21. L. Devkota, C.-M. Lin, T. E. Strecker, Y. Wang, J. K. Tidmore, Z. Chen, R. Guddneppanavar, C. J. Jelinek, R. Lopez, L. Liu, E. Hamel, R. P. Mason, D. J. Chaplin, M. L. Trawick and K. G. Pinney, *Bioorg. Med. Chem.*, 2016, **24**, 938–956.
22. R. P. Tanpure, B. L. Nguyen, T. E. Strecker, S. Aguirre, S. Sharma, D. J. Chaplin, B. G. Siim, E. Hamel, J. W. Lippert, G. R. Pettit, M. L. Trawick and K. G. Pinney, *J. Nat. Prod.*, 2011, **74**, 1568–1574.
23. R. P. Tanpure, C. S. George, T. E. Strecker, L. Devkota, J. K. Tidmore, C.-M. Lin, C. A. Herdman, M. T. MacDonough, M. Sriram, D. J. Chaplin, M. L. Trawick and K. G. Pinney, *Bioorg. Med. Chem.*, 2013, **21**, 8019–8032.
24. C. A. Herdman, L. Devkota, C.-M. Lin, H. Niu, T. E. Strecker, R. Lopez, L. Liu, C. S. George, R. P. Tanpure, E. Hamel, D. J. Chaplin, R. P. Mason, M. L. Trawick and K. G. Pinney, *Bioorg. Med. Chem.*, 2015, **23**, 7497–7520.
25. M. Sriram, J. J. Hall, N. C. Grohmann, T. E. Strecker, T. Wootton, A. Franken, M. L. Trawick and K. G. Pinney, *Bioorg. Med. Chem.*, 2008, **16**, 8161–8171.
26. R. P. Tanpure, C. S. George, M. Sriram, T. E. Strecker, J. K. Tidmore, E. Hamel, A. K. Charlton-Sevcik, D. J. Chaplin, M. L. Trawick and K. G. Pinney, *MedChemComm*, 2012, **3**, 720–724.
27. K. Nakata, Y. Sano and I. Shiina, *Mol. Basel*, 2010, **15**, 6773–6794.
28. S. M. Scholl, K. K. Huff and M. E. Lippman, *Endocrinology*, 1983, **113**, 611–617.
29. C. A. Herdman, T. E. Strecker, R. P. Tanpure, Z. Chen, A. Winters, J. Gerberich, L. Liu, E. Hamel, R. P. Mason, D. J. Chaplin, M. Lynn Trawick and K. G. Pinney, *MedChemComm*, 2016, **7**, 2418–2427.

30. R. P. Tanpure, A. R. Harkrider, T. E. Strecker, E. Hamel, M. L. Trawick and K. G. Pinney, *Bioorg. Med. Chem.*, 2009, **17**, 6993–7001.
31. D. W. Siemann, D. J. Chaplin and M. R. Horsman, *Cancer*, 2004, **100**, 2491–2499.
32. J. Denekamp, S. A. Hill and B. Hobson, *Eur. J. Cancer Clin. Oncol.*, 1983, **19**, 271–275.
33. G. M. Tozer, C. Kanthou and B. C. Baguley, *Nat. Rev. Cancer*, 2005, **5**, 423–435.
34. J. Mattern and M. Volm, *Cytotechnology*, 1998, **27**, 249–256.
35. M. R. Horsman, A. B. Bohn and M. Busk, *Exp. Oncol.*, 2010, **32**, 143–148.
36. C. Kanthou and G. M. Tozer, *Int. J. Exp. Pathol.*, 2009, **90**, 284–294.
37. R. A. Stanton, K. M. Gernert, J. H. Nettles and R. Aneja, *Med. Res. Rev.*, 2011, **31**, 443–481.
38. R. P. Mason, D. Zhao, L. Liu, M. L. Trawick and K. G. Pinney, *Integr. Biol.*, 2011, **3**, 375–387.
39. P. E. Thorpe, *Clin. Cancer Res.*, 2004, **10**, 415–427.
40. N. Ferrara, K. J. Hillan and W. Novotny, *Biochem. Biophys. Res. Commun.*, 2005, **333**, 328–335.
41. D. Zhao, E. Richer, P. P. Antich and R. P. Mason, *FASEB J. Off. Publ. Fed. Am. Soc. Exp. Biol.*, 2008, **22**, 2445–2451.
42. M. Folaron and M. Seshadri, *Mol. Imaging Biol. MIB Off. Publ. Acad. Mol. Imaging*, 2016, **18**, 860–869.
43. E. Hamel, *Cell Biochem. Biophys.*, 2003, **38**, 1–21.
44. D. W. Siemann, *Cancer Treat. Rev.*, 2011, **37**, 63–74.
45. P. Vaupel, F. Kallinowski and P. Okunieff, *Cancer Res.*, 1989, **49**, 6449–6465.
46. M. R. Horsman, *Int. J. Hyperthermia*, 2008, **24**, 57–65.
47. G. R. Pettit, A. Thornhill, N. Melody and J. C. Knight, *J. Nat. Prod.*, 2009, **72**, 380–388.
48. D. W. Siemann, D. J. Chaplin and P. A. Walicke, *Expert Opin. Investig. Drugs*, 2009, **18**, 189–197.
49. K. G. Pinney, V. P. Mocharla, Z. Chen, C. M. Garner, A. Ghatak, M. Hadimani, J. Kessler, J. M. Dorsey, K. Edvardsen, D. J. Chaplin, J. Prezioso, U. R. Ghatak, US20040043969 A1, 2004.
50. A. R. Shirali, "Inhibitors of Tubulin Assembly: Designed Ligands Featuring Benzo[b]thiophene, Dihydronaphthalene and Aroylchromene Molecular Core Structure." Dissertation, Baylor University, 2002.

51. M. B. Hadimani, "Studies Toward the Discovery of New Classes of Privileged Molecules as Colchicine-Site Binding Ligands for Tubulin: Structure-Based Design, Synthesis, and Bioactivity of Small Ligands Targeted at Tumor Vasculature." Dissertation, Baylor University, 2004.
52. A. Dogra, "Design and Synthesis of Dihydronaphthalene Vascular Disrupting Agents and Indolequinone-Based Bioreductives." Master's Thesis, Baylor University, 2006.
53. C. J. Jelinek, "Discovery and Development of Dihydronaphthalene-Based Vascular Targeting Agents and Combretastatin-Related Analogs." Master's Thesis, Baylor University, 2004.
54. E. Rasolofonjatovo, O. Provot, A. Hamze, J. Rodrigo, J. Bignon, J. Wdzieczak-Bakala, D. Desravines, J. Dubois, J. D. Brion and M. Alami, *Eur. J. Med. Chem.*, 2012, **52**, 22–32.
55. G. R. Pettit, B. Toki, D. L. Herald, P. Verdier-Pinard, M. R. Boyd, E. Hamel and R. K. Pettit, *J. Med. Chem.*, 1998, **41**, 1688–1695.
56. G. R. Pettit, M. P. Grealish, D. L. Herald, M. R. Boyd, E. Hamel and R. K. Pettit, *J. Med. Chem.*, 2000, **43**, 2731–2737.
57. R. Pettit and M. R. Rhodes, WO1999035150A1, 1999.
58. G. R. Pettit and M. R. Rhodes, *Anticancer. Drug Des.*, 1998, **13**, 183–191.
59. G. R. Pettit and J. W. Lippert, *Anticancer. Drug Des.*, 2000, **15**, 203–216.
60. I. Pravst, M. Zupan and S. Stavber, *Tetrahedron Lett.*, 2006, **47**, 4707–4710.
61. A. Ghatak, J. M. Dorsey, C. M. Garner and K. G. Pinney, *Tetrahedron Lett.*, 2003, **44**, 4145–4148.
62. A. Darwish and J. M. Chong, *J. Org. Chem.*, 2007, **72**, 1507–1509.
63. Shagufta, R. Raghunandan, P. R. Maulik and G. Panda, *Tetrahedron Lett.*, 2005, **46**, 5337–5341.
64. W. Liang, Y. Ni and F. Chen, *Oncotarget*, 2016, **7**, 15444–15459.
65. L. Liu, H. Beck, X. Wang, H.-P. Hsieh, R. P. Mason and X. Liu, *PLOS ONE*, 2012, **7**, e43314.
66. M. K. Alhasan, L. Liu, M. A. Lewis, J. Magnusson and R. P. Mason, *PLOS ONE*, 2012, **7**, e46106.
67. P. Zhang, Y. Chen, J. Liu, Y. Yang, Q. Lv, J. Wang, L. Zhang and M. Xie, *Ultrasound Med. Biol.*, 2018, **44**, 840–852.

68. M. Sriram, "Design, Synthesis, Biochemical and Biological Evaluation of Benzocyclic and Eneidyne Analogs of Combretastatins as Potential Tubulin Binding Ligands in the Treatment of Cancer." Dissertation, Baylor University, 2007.
69. R. Siles, J. F. Ackley, M. B. Hadimani, J. J. Hall, B. E. Mugabe, R. Guddneppanavar, K. A. Monk, J.-C. Chapuis, G. R. Pettit, D. J. Chaplin, K. Edvarlsen, M. L. Trawick, C. M. Garner and K. G. Pinney, *J. Nat. Prod.*, 2008, **71**, 313–320.
70. V. Vichai and K. Kirtikara, *Nat. Protoc.*, 2006, **1**, 1112–1116.
71. A. Monks, D. Scudiero, P. Skehan, R. Shoemaker, K. Paull, D. Vistica, C. Hose, J. Langley, P. Cronise and A. Vaigro-Wolff, *J. Natl. Cancer Inst.*, 1991, **83**, 757–766.
72. E. Hamel and C. M. Lin, *Biochim. Biophys. Acta BBA - Gen. Subj.*, 1981, **675**, 226–231.
73. H. Zhou, Z. Zhang, R. Denney, J. S. Williams, J. Gerberich, S. Stojadinovic, D. Saha, J. M. Shelton and R. P. Mason, *Oncotarget*, 2017, **8**, 37464–37477.
74. D. W. Siemann, D. J. Chaplin and M. R. Horsman, *Cancer Invest.*, 2017, **35**, 519–534.
75. D. W. Siemann, M. C. Bibby, G. G. Dark, A. P. Dicker, F. A. L. M. Eskens, M. R. Horsman, D. Marmé and P. M. Lorusso, *Clin. Cancer Res. Off. J. Am. Assoc. Cancer Res.*, 2005, **11**, 416–420.
76. G. M. Tozer, V. E. Prise, J. Wilson, M. Cemazar, S. Shan, M. W. Dewhurst, P. R. Barber, B. Vojnovic and D. J. Chaplin, *Cancer Res.*, 2001, **61**, 6413–6422.
77. G. M. Tozer, C. Kanthou, C. S. Parkins and S. A. Hill, *Int. J. Exp. Pathol.*, 2002, **83**, 21–38.

Table of Contents entry (Graphical Abstract)

Dihydronaphthalene Analogues as Potent Inhibitors of Tubulin Polymerization, Cytotoxic Agents, and Vascular Disrupting Agents (VDAs).